bioRxiv preprint doi: https://doi.org/10.1101/2022.12.20.521163; this version posted April 18, 2023. The copyright holder for this preprint (which was not certified by peer review) is the author/funder, who has granted bioRxiv a license to display the preprint in perpetuity. It is made available under aCC-BY 4.0 International license.

1 **pGG-PIP: A GreenGate (GG) entry vector collection with Plant Immune system Promoters**
2 **(PIP)**

3 Jacob Calabria[1,2,a], Madlen I. Rast-Somssich[2,5,b,#], Liu Wang[1,3,6,c,#], Hsiang-Wen Chen[1,3,d],
4 Michelle Watt[2,e], Alexander Idnurm[4,f], Staffan Persson[3,6,g], and Marc Somssich[1,7,h,*]

5 [1] Plant-Fusarium Interactions Research Team, School of BioSciences, University of Melbourne, Parkville, Australia
6 [2] Crop Root Physiology Lab, School of BioSciences, University of Melbourne, Parkville, Australia
7 [3] Plant Cell Biology Lab, School of BioSciences, University of Melbourne, Parkville, Australia
8 [4] Mycology Laboratory, School of BioSciences, University of Melbourne, Parkville, Australia
9 [5] Current address: Institute for Molecular Physiology, Heinrich Heine University, Düsseldorf, Germany
10 [6] Current address: Copenhagen Plant Science Center, University of Copenhagen, Frederiksberg C, Denmark
11 [7] Current address: Max Planck Institute for Plant Breeding Research, Cologne, Germany
12 Twitter: [a] @jacobcalabria, [b] @MSomssich, [c] @Liu_Wang1, [d] @HsiangWen_Chen, [e] @MelbourneRoots, [f]
13 @AlexanderIdnurm, [g] @perssonlab1, [h] @somssichm
14 [#] These two authors contributed equally
15 [*] For correspondence: marc.somssich@unimelb.edu.au

16 **Abstract**

17 The regulatory sequences controlling the expression of a gene (i.e., the promoter) are essential to
18 properly understand a gene's function. From their use in mutant complementation assays, to
19 studying their responsiveness to different stimuli via transcriptional reporter lines or using them
20 as proxy for the activation of certain pathways, assays using promoter sequences are valuable tools
21 for insight into the genetic architecture underlying plant life. The GreenGate (GG) system is a
22 plant-specific variant of the Golden Gate assembly method, a modular cloning system that allows
23 the hierarchical assembly of individual donor DNA fragments into one expression clone via a
24 single reaction step. Here, we present a collection of 75 GG entry vectors carrying putative
25 regulatory sequences for *Arabidopsis thaliana* genes involved in many different pathways of the
26 plant immune system, designated Plant Immune system Promoters (PIP). This pGG-PIP entry
27 vector set enables the rapid assembly of expression vectors to be used for transcriptional reporters
28 of plant immune system components, mutant complementation assays when coupled with coding
29 sequences, mis-expression experiments for genes of interest, or the targeted use of CRISPR/Cas9
30 genome editing. We used pGG-PIP vectors to create fluorescent transcriptional reporters in *A.*
31 *thaliana* and demonstrated the potential of these reporters to image the responsiveness of specific

bioRxiv preprint doi: https://doi.org/10.1101/2022.12.20.521163; this version posted April 18, 2023. The copyright holder for this preprint (which was not certified by peer review) is the author/funder, who has granted bioRxiv a license to display the preprint in perpetuity. It is made available under aCC-BY 4.0 International license.

32 plant immunity genes to infection and colonization by the fungal pathogen *Fusarium oxysporum*.
33 Using the PLANT ELICITOR PEPTIDE (PEP) pathway as an example, we show that several
34 components of this pathway are locally activated in response to colonization by the fungus.

35 **Keywords**

36 Golden Gate; GreenGate; plant immunity; *Arabidopsis thaliana*; plant-microbe interactions;
37 promoters; transcriptional reporters; PLANT ELICITOR PEPTIDE; synthetic biology; *Fusarium*
38 *oxysporum*

39 Introduction

40 Since the development of molecular cloning in the early 1970s, the isolation of genes and
41 promoters, and subsequent transgenesis of model organisms, has become standard practice in the
42 life sciences (Somssich, 2022). The development of more advanced cloning methods, particularly
43 the recombination-based Gateway technology in the year 2000, made the creation of expression
44 clones ready for transformation ever easier (Hartley *et al.*, 2000). However, with the rise of the
45 synthetic biology field, it is now no longer sufficient for these methods to facilitate the cloning of
46 individual DNA fragments. To recreate entire pathways and gene circuits in plants and other model
47 organisms, larger DNA constructs need to be readily assembled from individual components, and
48 these distinct building blocks need to be compatible to allow the flexibility to mix and match
49 different promoters, coding sequences, protein tags, terminators, and resistance genes for selection
50 of transgenic lines (Meng and Ellis, 2020). This requirement was met with the new modular
51 cloning techniques which use recombination-based hierarchical assembly of multiple donor-
52 modules (each containing, for example, a promoter of choice, tag of choice, gene of interest, etc.)
53 into one ordered expression clone to be used for transgenesis (Fig. 1) (Bird *et al.*, 2022). Among
54 the developed modular cloning methods, the Golden Gate system has emerged as the most widely
55 utilized version, and in 2013 Lampropoulos *et al.* developed the plant-specific GreenGate variant
56 of the Golden Gate technique (Engler *et al.*, 2008, 2009; Weber *et al.*, 2011; Lampropoulos *et al.*,
57 2013). The GreenGate toolkit provides users with a wide range of entry vectors that serve as donors
58 for standard promoters (e.g. CaMV35S, UBQ10), protein tags (e.g. GFP, NLS, HDEL),
59 terminators (e.g. CaMV35S, UBQ10) and plant resistance cassettes (e.g. BastaR, HygR, KanR),
60 to build basic gene expression modules for plants.

bioRxiv preprint doi: https://doi.org/10.1101/2022.12.20.521163; this version posted April 18, 2023. The copyright holder for this preprint (which was not certified by peer review) is the author/funder, who has granted bioRxiv a license to display the preprint in perpetuity. It is made available under aCC-BY 4.0 International license.

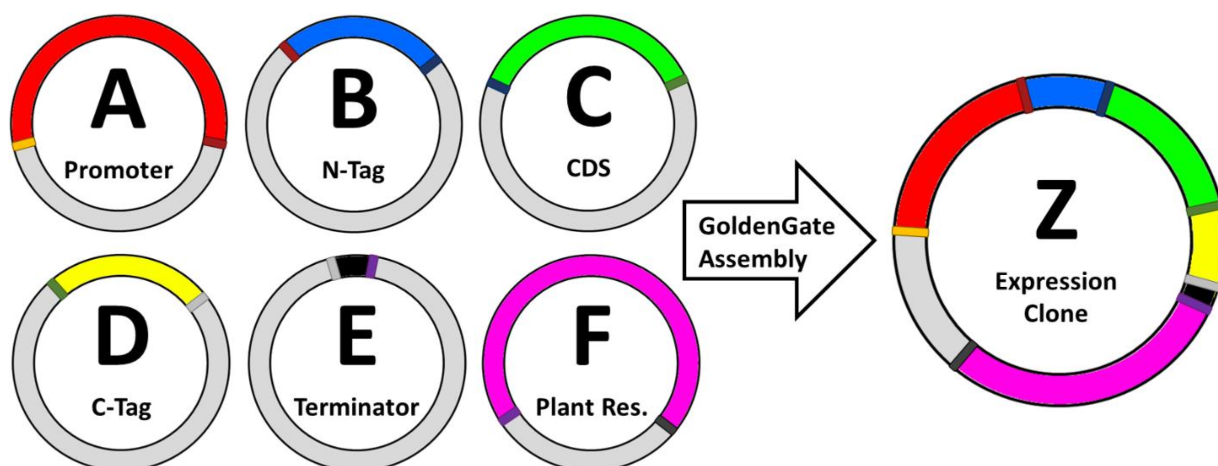

Figure 1: Overview of the modular Golden/GreenGate cloning principle
The promoter, N- and C-terminal tags, the gene-of-interest coding sequence (CDS), a terminator, and a plant resistance cassette are all cloned into individual entry clones (A-F), which are then combined with an 'empty' destination clone (Z) in the Golden Gate assembly mix. During the assembly reaction, the *Bsa*I restriction enzyme cuts the different fragments from their respective entry clones. These fragments subsequently self-align via complementary four base pair overhangs (indicated by the thin colored borders on each entry vector; complementary overhangs that will align have the same color), and the T4 DNA-ligase fuses the individual fragments in the final expression clone (Z) that can be used to transform plants.

61 Additional kits have been developed and added to the GreenGate toolbox since 2013, providing
62 entry vector sets to build plasmids for CRISPR/Cas9-guided genome editing (Wu *et al.*, 2018),
63 CRISPR/Cas9-guided tissue-specific gene knockout (Decaestecker *et al.*, 2019) and inducible and
64 cell-type specific gene expression (Schürholz *et al.*, 2018). In addition, a toolbox of fluorescent
65 proteins suitable for work in plants (Denay *et al.*, 2019), along with the necessary clones for *in*
66 *planta* proximity ligation assays using the biotin ligase (Goslin *et al.*, 2021), and destination
67 vectors with an already integrated plasma membrane-marker (Kümpers *et al.*, 2022) have been
68 designed. The development and availability of these various toolboxes, all compatible with each
69 other, demonstrate the usefulness of such modular systems to enable researchers to quickly adopt
70 new technologies, providing the flexibility and versatility to combine and recombine their existing
71 vectors (i.e., modules) with new vectors from all other kits.

72 In our work we use a microscopy-based live-imaging approach to monitor the *Arabidopsis*
73 *thaliana*'s defense responses to infection and colonization by the pathogenic fungus *Fusarium*
74 *oxysporum* strain *Fo*5176 (*Fo*5176) on an individual cell level (Calabria *et al.*, 2022; Wang *et al.*,
75 2022*a*). Fluorescent transcriptional reporters are a good tool for such studies, as activation of
76 certain pathways is typically associated with transcriptional upregulation (Ngou *et al.*, 2021).
77 However, most studies investigating the transcriptional responsiveness of certain pathways to

bioRxiv preprint doi: https://doi.org/10.1101/2022.12.20.521163; this version posted April 18, 2023. The copyright holder for this preprint (which was not certified by peer review) is the author/funder, who has granted bioRxiv a license to display the preprint in perpetuity. It is made available under aCC-BY 4.0 International license.

78 pathogens tend to use transcriptomic analyses of whole tissues, organs, or seedlings, therefore
79 losing all spatial resolution and differences between cell groups and even individual cells. The
80 responses of only the few cells that could be the major contributors to a host-microbe outcome are
81 also typically lost in such experiments, as they are below the threshold of background noise. A
82 microscopy-based approach that allows for the spatial resolution and observation of responses in
83 individual cells therefore closes this knowledge gap. One reason why such an approach is not more
84 common is that a prerequisite for this work is the availability of fluorescent reporter lines for all
85 the different plant immune pathways to be investigated. To this end, we have cloned the putative
86 regulatory sequences (i.e., promoters) of 75 *A. thaliana* genes, representing many of the major
87 branches of the plant immune system (Fig. 2 and Table 1). We have done so using the GreenGate
88 cloning system, therefore creating a GreenGate plant promoter entry vector set that is compatible
89 with all other GreenGate-based toolkits, and that we believe will be a valuable tool for the scientific
90 community.

91 As a proof-of-principle, we selected a number of these promoters to create fluorescent
92 transcriptional reporter lines for genes involved in the PLANT ELICITOR PEPTIDE (PEP)-
93 pathway. The PEP pathway is involved in the immune response to several plant pathogens,
94 including bacteria, fungi and oomycetes (Saijo *et al.*, 2018). The PEP1-6 peptides function as
95 phytosulfokines. They are expressed as part of the plant's pattern-triggered immunity (PTI)
96 response and trigger cell autonomous and non-autonomous defense responses when they are
97 perceived by the plasma membrane localized receptors PEPR1 and PEPR2 (Yamaguchi *et al.*,
98 2006, 2010; Saijo *et al.*, 2018). For their function, they require the intracellular kinase BIK1, which
99 activates the NADPH oxidase RBOHD to trigger a ROS-burst, and also induces defense gene
100 expression (Liu *et al.*, 2013; Kadota *et al.*, 2014; Saijo *et al.*, 2018; Jing *et al.*, 2020). A role for
101 the PEP pathway in the defense against fungal disease has been hypothesized, based on large-scale
102 transcriptomic data. Plants carrying mutations in *MEDIATOR18* and *20* show increased resistance
103 to infection by *F. oxysporum* strain *Fo*5176, and mRNA sequencing has demonstrated that *PEP1*
104 is among the genes no longer induced after infection of these mutant plants (Fallath *et al.*, 2017;
105 Wang *et al.*, 2022*a*). Similarly, *PEPR1* and *2* were among the genes suppressed by the endophytic
106 *F. oxysporum* strain *Fo*47, indicating that the PEP pathway normally acts to restrict fungal
107 colonization (Guo *et al.*, 2021; Wang *et al.*, 2022*a*). However, no detailed data is available. Here,
108 we show that colonization of the *A. thaliana* vasculature is accompanied by a highly localized

bioRxiv preprint doi: https://doi.org/10.1101/2022.12.20.521163; this version posted April 18, 2023. The copyright holder for this preprint (which was not certified by peer review) is the author/funder, who has granted bioRxiv a license to display the preprint in perpetuity. It is made available under aCC-BY 4.0 International license.

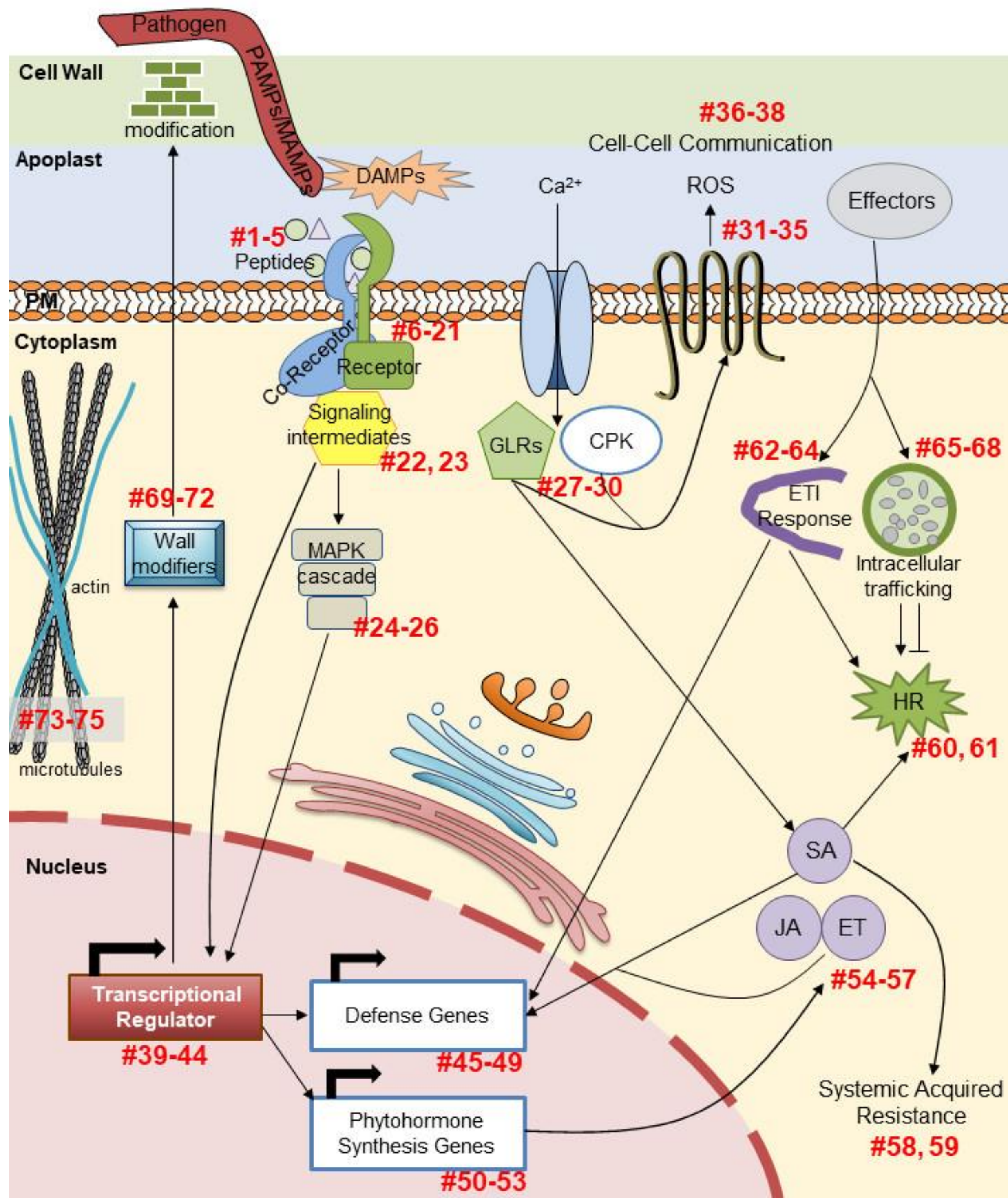

Figure 2: Overview of the different immune pathways represented in the pGG-PIP collection
The red numbers correspond to the pGG-PIP plasmid numbers in column one of Table 1.

109 activation of this pathway via upregulation of genes encoding the peptide ligand PEP1, as well as
110 the cognate PEP RECEPTORs 1 and 2, the downstream signaling intermediate BIK1 and the
111 NADPH oxidase RBOHD.

bioRxiv preprint doi: https://doi.org/10.1101/2022.12.20.521163; this version posted April 18, 2023. The copyright holder for this preprint (which was not certified by peer review) is the author/funder, who has granted bioRxiv a license to display the preprint in perpetuity. It is made available under aCC-BY 4.0 International license.

112 **Results**

113 **Selection and cloning of the promoters**

114 By using these putative promoter sequences for the construction of transcriptional reporter lines,
115 our main aim is to obtain information about the specific localized activation of different immune
116 pathways in response to infection by a pathogen, in our case *Fo*5176. Once we have identified
117 pathways involved in the plant's defense against this strain, we plan to further extend these
118 experiments based on what is known about the function of these pathways. Thus, it is important to
119 select promoters from many different pathways of the plant immune system, but also from
120 pathways that are particularly well understood, since this existing knowledge will guide our future
121 work. Some of the best studied immune pathways in the plant are the pattern-recognition flagellin
122 (flg) and elongation factor thermos unstable (EF-Tu) pathways, the phytohormones jasmonic acid
123 (JA), salicylic acid (SA) and ethylene (ET), and the transcriptional activity of several WRKY
124 transcription factors. We therefore selected representative gene promoters from such well
125 understood pathways, but also additional candidates such as MAP and calcium-dependent protein
126 kinases (MPKs, CPKs), genes involved in production and signaling via reactive oxygen species
127 (ROS), and genes involved in effector-triggered immunity (ETI) responses via the EDS1-PAD4
128 module. Figure 2 and Table 1 provide a complete overview of the 75 promoters included in the
129 pGG-PIP collection. The numbers in Fig. 2 correspond to the pGG-PIP plasmid number in the first
130 column of Table 1.

131 For the construction of the pGG-PIP plasmids, we considered the entire stretch of DNA from the
132 3´ upstream neighboring gene's coding sequence to the ATG of the gene of interest as the gene's
133 putative regulatory sequences, and thus its 'promoter'. There are a few exceptions to this rule,
134 where we used a defined stretch of DNA that has previously been described to complement a
135 mutant (e.g., *FMO1*, *RPS4* (Wirthmueller *et al.*, 2007; Joglekar *et al.*, 2018)). Where present, this
136 may include untranslated regions (UTRs), pseudogenes, or transposons, since these elements could
137 indeed affect expression of a gene *in planta*. For the recombination-based cloning, the *Bsa*I
138 recognition site and standard four base pair GreenGate A overhangs (5´-ACCT and TTGT-3´)
139 were added via primers during amplification of the promoter sequences (see Supplementary Table
140 1 for a list of primer sequences). If the promoter sequence contained an internal *Bsa*I restriction
141 site (GGTCTC), we mutated a single base, usually a G to a C via scar-free *Bsa*I cloning, i.e., we

bioRxiv preprint doi: https://doi.org/10.1101/2022.12.20.521163; this version posted April 18, 2023. The copyright holder for this preprint (which was not certified by peer review) is the author/funder, who has granted bioRxiv a license to display the preprint in perpetuity. It is made available under aCC-BY 4.0 International license.

142 inserted the base mutation by making it part of the four base pair overhang used for the scar-free
143 cloning (see Table 1 for the exact sequence edits made, and Supplementary Table 1 for primer
144 sequences). The promoters were then transferred into the GreenGate promoter entry vector
145 pGGA000 via the four base pair A overhangs in a Golden Gate assembly reaction.

GG-PIP plasmid	Gene	Bases	*Bsa*I site edits	Protein function	Full gene name	Gene code
pGG-PIP01	*PEP1*	1907		Activate defense genes (Yamada *et al.*, 2016)	*PLANT ELICITOR PEPTIDE 1*	*AT5G64900*
pGG-PIP02	*PEP2*	769		Activate defense genes (Yamada *et al.*, 2016)	*PLANT ELICITOR PEPTIDE 2*	*AT5G64890*
pGG-PIP03	*PEP3*	1694		Activate defense genes (Yamada *et al.*, 2016)	*PLANT ELICITOR PEPTIDE 3*	*AT5G64905*
pGG-PIP04	*RALF23*	2027	1458 C -> G	Phytosulfokine sensed by FER (Stegmann *et al.*, 2017)	*ARABIDOPSIS RAPID ALKALINIZATION FACTOR 23*	*AT3G16570*
pGG-PIP05	*SCOOP12*	2900		Phytosulfokine sensed by MIK2/BAK1 (Hou *et al.*, 2021; Rhodes *et al.*, 2021)	*PRECURSOR OF SERINE-RICH ENDOGENOUS PEPTIDE 12*	*AT5G44585*
pGG-PIP06	*BAK1*	1731		Co-receptor for several defense & development pathways (Greenwood and Williams, 2022)	*BRI1-ASSOCIATED RECEPTOR KINASE*	*AT4G33430*
pGG-PIP07	*CERK1*	493		Chitin-receptor (Cao *et al.*, 2014)	*CHITIN ELICITOR RECEPTOR KINASE 1*	*AT3G21630*
pGG-PIP08	*CIPP1*	3003		CERK1 co-receptor (Liu *et al.*, 2018)	*CERK-1 INTERACTING PROTEIN PHOSPHATASE 1*	*AT1G34750*
pGG-PIP09	*CORK1*	3376		DAMP-receptor (Tseng *et al.*, 2022)	*CELLOOLIGOMER RECEPTOR KINASE 1*	*AT1G56145*
pGG-PIP10	*EFR*	2376		Receptor for EF-Tu (Couto and Zipfel, 2016)	*EF-TU RECEPTOR*	*AT5G20480*
pGG-PIP11	*FER*	1243		Co-receptor for several defense & development pathways (Duan *et al.*, 2022)	*FERONIA*	*AT3G51550*
pGG-PIP12	*FLS2*	2913		Receptor for bacterial flagellin (Couto and Zipfel, 2016)	*FLAGELLIN-SENSITIVE 2*	*AT5G46330*
pGG-PIP13	*LYK5*	1560	1215 G->C	CERK1 co-receptor (Cao *et al.*, 2014)	*LYSM-CONTAINING RECEPTOR-LIKE KINASE 5*	*AT2G33580*
pGG-PIP14	*LYM1*	991		Fungal MAMP receptor (Zipfel and Oldroyd, 2017)	*LYSM DOMAIN GPI-ANCHORED PROTEIN 1 PRECURSOR*	*AT1G21880*
pGG-PIP15	*MIK2*	2513		SCOOP peptide receptor (Hou *et al.*, 2021; Rhodes *et al.*, 2021)	*MALE DISCOVERER 1-INTERACTING RECEPTOR-LIKE KINASE 2*	*AT4G08850*
pGG-PIP16	*PEPR1*	931	180 G->A	Receptor for PEP1-6 (Yamada *et al.*, 2016)	*PEP1 RECEPTOR 1*	*AT1G73080*
pGG-PIP17	*PEPR2*	1676		Receptor for PEP1 & 2 (Yamada *et al.*, 2016)	*PEP1 RECEPTOR 2*	*AT1G17750*
pGG-PIP18	*RFO1*	850		Cell wall-associated kinase (Huerta *et al.*, 2023)	*RESISTANCE TO FUSARIUM OXYSPORUM 1*	*AT1G79670*
pGG-PIP19	*RLP26*	822		Co-receptor for PRR receptors (Wu *et al.*, 2016)	*RECEPTOR LIKE PROTEIN 26*	*AT2G33050*
pGG-PIP20	*RLP29*	2790		Co-receptor for PRR receptors (Wu *et al.*, 2016)	*RECEPTOR LIKE PROTEIN 29*	*AT2G42800*
pGG-PIP21	*SOBIR1*	1163		Co-receptor for several defense pathways (Cho *et al.*, 2022)	*SUPPRESSOR OF BIR 1 / EVERSHED*	*AT2G31880*
pGG-PIP22	*BIK1*	2668		Defense signaling (Gonçalves Dias *et al.*, 2022)	*BOTRYTIS-INDUCED KINASE1*	*AT2G39660*
pGG-PIP23	*XLG2*	1256		G protein involved in immunity (Petutschnig *et al.*, 2022)	*EXTRA-LARGE GTP-BINDING PROTEIN 2*	*AT4G34390*
pGG-PIP24	*MPK3*	654		Activates immune response (Tsuda and Somssich, 2015)	*MITOGEN-ACTIVATED PROTEIN KINASE 3*	*AT3G45640*
pGG-PIP25	*MPK4*	1025		Activates immune response (Tsuda and Somssich, 2015)	*MITOGEN-ACTIVATED PROTEIN KINASE 4*	*AT4G01370*

bioRxiv preprint doi: https://doi.org/10.1101/2022.12.20.521163; this version posted April 18, 2023. The copyright holder for this preprint (which was not certified by peer review) is the author/funder, who has granted bioRxiv a license to display the preprint in perpetuity. It is made available under aCC-BY 4.0 International license.

pGG-PIP26	*MPK6*	811		Activates immune response (Tsuda and Somssich, 2015)	*MITOGEN-ACTIVATED PROTEIN KINASE 6*	*AT2G43790*
pGG-PIP27	*CPK5*	1983		Involved in calcium-dependent stress responses (Gao and He, 2013)	*CALMODULIN-DOMAIN PROTEIN KINASE 5*	*AT4G35310*
pGG-PIP28	*CPK29*	826	325 G->C	Involved in calcium-dependent stress responses (Patil and Senthil-Kumar, 2020)	*CALCIUM-DEPENDENT PROTEIN KINASE 29*	*AT1G76040*
pGG-PIP29	*GLR2.5*	2488	1488, 1489 G->C	Involved in defense-development balancing (Birkenbihl *et al.*, 2017*a*)	*GLUTAMATE RECEPTOR 2.5*	*AT5G11210*
pGG-PIP30	*GLR2.7*	4000		Involved in defense-development balancing (Birkenbihl *et al.*, 2017*a*)	*GLUTAMATE RECEPTOR 2.7*	*AT2G29120*
pGG-PIP31	*RBOHD*	2309		Produces ROS-burst (Kadota *et al.*, 2014)	*RESPIRATORY BURST OXIDASE HOMOLOGUE D*	*AT5G47910*
pGG-PIP32	*RBOHF*	4119		Produces ROS-burst (Morales *et al.*, 2016)	*RESPIRATORY BURST OXIDASE HOMOLOG F*	*AT1G64060*
pGG-PIP33	*EX1*	989		Produces ROS from chloroplasts (Dogra *et al.*, 2022)	*EXECUTER 1*	*AT4G33630*
pGG-PIP34	*HPCA1*	2944		ROS-sensor (Sun and Zhang, 2021)	*HP-INDUCED Ca2+ INCREASES 1*	*AT5G49760*
pGG-PIP35	*RCD1*	3137	2888 G -> C	Modulator of root-to-shoot ROS-signaling (Jin *et al.*, 2022)	*RADICAL-INDUCED CELL DEATH1*	*AT1G32230*
pGG-PIP36	*DORN1*	2325		eATP DAMP-receptor (Sun and Zhang, 2021)	*DOES NOT RESPOND TO NUCLEOTIDES 1*	*AT5G60300*
pGG-PIP37	*LECRK-VI.2*	1183		NAD(P)-receptor (Sun and Zhang, 2021)	*L-TYPE LECTIN RECEPTOR KINASE-VI.2*	*AT5G01540*
pGG-PIP38	*BPS1*	2142		Regulator of root-to-shoot communication (Lee *et al.*, 2016)	*BYPASS 1*	*AT1G01550*
pGG-PIP39	*WRKY11*	2026	240 C->G	Regulates defense gene expression (Journot-Catalino *et al.*, 2006)	*WRKY DNA-BINDING PROTEIN 11*	*AT4G31550*
pGG-PIP40	*WRKY17*	4565	4325 G->C	Regulates defense gene expression (Birkenbihl *et al.*, 2018)	*WRKY DNA-BINDING PROTEIN 17*	*AT2G24570*
pGG-PIP41	*WRKY33*	1665		Regulates defense gene expression (Birkenbihl *et al.*, 2018)	*WRKY DNA-BINDING PROTEIN 33*	*AT4G23810*
pGG-PIP42	*WRKY40*	4158		Regulates defense gene expression (Birkenbihl *et al.*, 2018)	*WRKY DNA-BINDING PROTEIN 40*	*AT1G80840*
pGG-PIP43	*WRKY53*	2515		Regulates defense gene expression (Birkenbihl *et al.*, 2017*b*)	*WRKY DNA-BINDING PROTEIN 53*	*AT2G38470*
pGG-PIP44	*WRKY70*	4099		Regulates defense gene expression (Journot-Catalino *et al.*, 2006)	*WRKY DNA-BINDING PROTEIN 70*	*AT3G56400*
pGG-PIP45	*ELI-3*	524		Elicitor-response gene (Tanaka *et al.*, 2018)	*CINNAMYL-ALCOHOL DEHYDROGENASE 7 / ELICITOR-ACTIVATED GENE3*	*AT4G37980*
pGG-PIP46	*FRK1*	1271		Defense gene (Birkenbihl *et al.*, 2017*b*)	*FLG22-INDUCED RECEPTOR-LIKE KINASE 1*	*AT2G19190*
pGG-PIP47	*MLO6*	3042		Defense gene (Acevedo-Garcia *et al.*, 2017)	*MILDEW RESISTANCE LOCUS O 6*	*AT1G61560*
pGG-PIP48	*PER5*	2007	558 C->G	Marker for activated immune signalling (Chuberre *et al.*, 2018)	*PEROXIDASE 5*	*AT1G14550*
pGG-PIP49	*PLP1*	2490		Pathogen-induced (Yang *et al.*, 2007)	*PATATIN-LIKE PROTEIN 1*	*AT4G37070*
pGG-PIP50	*ACS2*	2914	150 C->G	ET biosynthesis (Wang *et al.*, 2022*c*)	*1-AMINO-CYCLOPROPANE-1-CARBOXYLATE SYNTHASE 2*	*AT1G01480*
pGG-PIP51	*AOS*	2093	2088 G->C ;	JA biosynthesis (Yang *et al.*, 2019)	*ALLENE OXIDE SYNTHASE*	*AT5G42650*

bioRxiv preprint doi: https://doi.org/10.1101/2022.12.20.521163; this version posted April 18, 2023. The copyright holder for this preprint (which was not certified by peer review) is the author/funder, who has granted bioRxiv a license to display the preprint in perpetuity. It is made available under aCC-BY 4.0 International license.

			1434 G->C			
pGG-PIP52	*ARR5*	2229	639 C -> G	Cytokinin signaling (Lee *et al.*, 2016)	*ARABIDOPSIS RESPONSE REGULATOR 5*	*AT3G48100*
pGG-PIP53	*EDS16*	2975	1579 G->C ; 1049 C->G	SA biosynthesis (Calabria *et al.*, 2022)	*ENHANCED DISEASE SUSCEPTIBILITY TO ERYSIPHE ORONTII 16*	*AT1G74710*
pGG-PIP54	*ERF1*	2682		ET & JA response regulator (Wang *et al.*, 2022*c*)	*ETHYLENE RESPONSE FACTOR 1*	*AT3G23240*
pGG-PIP55	*PDF1.2*	1540		ET & JA-induced defense gene (Yang *et al.*, 2019)	*PLANT DEFENSIN 1.2*	*AT5G44420*
pGG-PIP56	*PR1*	2343		SA-induced defense gene (Yang *et al.*, 2019)	*PATHOGENESIS-RELATED GENE 1*	*AT2G14610*
pGG-PIP57	*VSP2*	1471		JA-induced defense gene (Yang *et al.*, 2019)	*VEGETATIVE STORAGE PROTEIN 2*	*AT5G24770*
pGG-PIP58	*FMO1*	1726		Systemic acquired resistance marker (Joglekar *et al.*, 2018)	*FLAVIN-DEPENDENT MONOOXYGENASE 1*	*AT1G19250*
pGG-PIP59	*MYB72*	4619		Involved in induced systemic resistance	*ARABIDOPSIS THALIANA MYB DOMAIN PROTEIN 72*	*AT1G56160*
pGG-PIP60	*CSLD2*	1963		Marker for cell death, possibly via ET-signaling (Salguero-Linares *et al.*, 2022)	*CELLULOSE-SYNTHASE LIKE D2*	*AT5G16910*
pGG-PIP61	*HRM1*	2238		Marker for cell death (Salguero-Linares *et al.*, 2022)	*HYPERSENSITIVE RESPONSE MARKER 1*	*AT5G17760*
pGG-PIP62	*EDS1*	1419	848 A->T ; 1269 G->C	Involved in ETI-signaling (Jia *et al.*, 2022)	*ENHANCED DISEASE SUSCEPTIBILITY 1*	*AT3G48090*
pGG-PIP63	*PAD4*	1596		Involved in ETI-signaling (Jia *et al.*, 2022)	*PHYTOALEXIN DEFICIENT 4*	*AT3G52430*
pGG-PIP64	*RPS4*	511		NLR effector receptor (Jia *et al.*, 2022)	*RESISTANT TO P. SYRINGAE 4*	*AT5G45250*
pGG-PIP65	*ATG8A*	1408		Autophagy marker (Yang *et al.*, 2018)	*AUTOPHAGY-RELATED 8A*	*AT4G21980*
pGG-PIP66	*TET8*	2068		Targets vesicular transport to infection sites (Cai *et al.*, 2018)	*TETRASPANIN8*	*AT2G23810*
pGG-PIP67	*SULTR4;1*	2087		Sulfate transporter (Wang *et al.*, 2022*b*)	*SULFATE TRANSPORTER 4.1*	*AT5G13550*
pGG-PIP68	*SULTR4;2*	712		Sulfate transporter (Wang *et al.*, 2022*b*)	*SULFATE TRANSPORTER 4.2*	*AT3G12520*
pGG-PIP69	*CAD5*	1134		Lignin biosynthesis (Kim *et al.*, 2020)	*CINNAMYL ALCOHOL DEHYDROGENASE 5*	*AT4G34230*
pGG-PIP70	*GPAT5*	1587		Suberin biosynthesis (Andersen *et al.*, 2015)	*GLYCEROL-3-PHOSPHATE SN-2-ACYLTRANSFERASE 5*	*AT3G11430*
pGG-PIP71	*MYB15*	2050		Lignin biosynthesis in response to pathogens (Kim *et al.*, 2020)	*ARABIDOPSIS THALIANA MYB DOMAIN PROTEIN 15*	*AT3G23250*
pGG-PIP72	*PMR4*	1954		PAMP-induced defense, callose-deposition (Blümke *et al.*, 2013)	*POWDERY MILDEW RESISTANT 4*	*AT4G03550*
pGG-PIP73	*FH16*	1158		Involved in microtubule/actin-network reorganisation (Wang *et al.*, 2013)	*FORMIN HOMOLOG 16*	*AT5G07770*
pGG-PIP74	*NET4A*	1718		Modulates the vacuole (Kaiser *et al.*, 2019)	*NETWORKED 4A*	*AT5G58320*
pGG-PIP75	*TUB6*	3349	2358 A->G	Component of microtubules (Liu *et al.*, 2019)	*BETA-6 TUBULIN*	*AT5G12250*

Table 1: List of the 75 pGG-PIP promoter entry vectors in the set described in this paper. The pGG-PIP numbers correspond to the red numbers in Fig. 2.

Using pGG-PIP vectors to create transcriptional reporters for the PEP pathway

To test the usefulness of these promoters to map local individual cell responses upon attack by a microbe, we created transcriptional reporter lines for genes involved in the PEP pathway. We used

bioRxiv preprint doi: https://doi.org/10.1101/2022.12.20.521163; this version posted April 18, 2023. The copyright holder for this preprint (which was not certified by peer review) is the author/funder, who has granted bioRxiv a license to display the preprint in perpetuity. It is made available under aCC-BY 4.0 International license.

151 a nuclear localized tandem of mTurqoise2 (mT2) fluorophores as a reporter, since mT2 has been
152 shown to be very bright and photostable in plant cells (Goedhart *et al.*, 2012; Long *et al.*, 2018;
153 Denay *et al.*, 2019). The nuclear localization enhances the brightness even further due to molecular
154 crowding, and furthermore helps to identify individual cells.

155 We first probed our reporters for the PEP1 and PEP2 peptides (pGG-PIP01 and 02), as well as the
156 PEPR1 and PEPR2 receptors (pGG-PIP16 and 17), assessing their local responsiveness to
157 colonization by *Fo*5176. Under control uninfected conditions, *PEP1* was weakly expressed in
158 inner tissue cells of the root differentiation zone (DZ) (Fig. S1A-D). No expression was detectable
159 in the root tip, the meristematic or elongation zones (MZ and EZ). *PEP2* was robustly expressed
160 in the DZ, but in contrast to *PEP1*, its expression was stronger in the outer tissues (Fig. S1G-H).
161 In addition, it was also expressed in the root tip, around the MZ and early EZ (Fig. S1E-F). *PEPR1*
162 was generally expressed at a very weak level. In the root tip, starting with the EZ, expression was
163 limited to the vasculature, while from the young DZ (or root hair zone) onward, expression was
164 restricted to the outer tissues (Fig. S2A-D). *PEPR2* was expressed only in the DZ, and only in the
165 vasculature, but expression was much stronger compared to *PEPR1* (Fig. S2E-H). Thus, in
166 vascular cells, *PEPR1* and *PEPR2* complemented each other under uninfected conditions.
167 Following colonization of the vasculature by *Fo*5176, *PEP1*, as well as both *PEPR*s, showed a
168 strong upregulation in the cells adjacent to the colonization site (Fig. 3). Interestingly, this

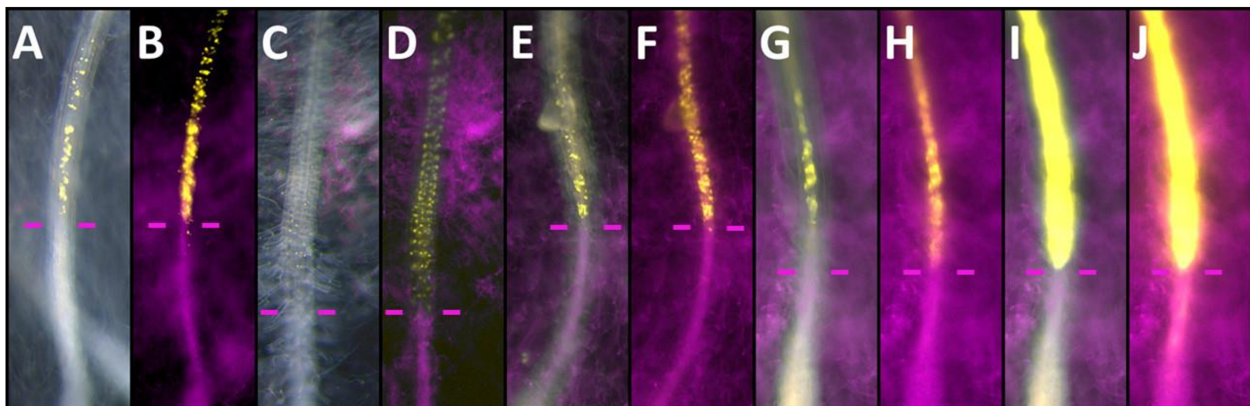

Figure 3: Local transcriptional responses in *PEP1*, *PEP2*, *PEPR1* and *PEPR2* expression to colonization by *Fo*5176
Bright field and fluorescence (**A, C, E, G, I**) and fluorescence only (**B, D, F, H, J**) images of colonized roots expressing the *PEP1* (A, B), *PEP2* (C, D), *PEPR1* (E, F) or *PEPR2* (G-J) reporters. *Fo*5176 is shown in magenta, the reporters in yellow. The purple bars indicate the fungal colonization front. All images were recorded with comparable imaging settings, except for G and H, which are the same as I and J, just with reduced exposure time. Expression of the *PEPR2* reporter was so strong (I, J), that we reduced the exposure time to visualize individual cells in G and H.

bioRxiv preprint doi: https://doi.org/10.1101/2022.12.20.521163; this version posted April 18, 2023. The copyright holder for this preprint (which was not certified by peer review) is the author/funder, who has granted bioRxiv a license to display the preprint in perpetuity. It is made available under aCC-BY 4.0 International license.

169 upregulation was limited to the cells of the vasculature, the exact tissue that is targeted and
170 colonized by *Fo*5176, showing how precisely the plant targets its response. Importantly, the
171 induction of *PEPR2* was much stronger than the induction of *PEP1* and *PEPR1* (Fig. 3G-J).
172 Interestingly, *PEP2* also showed an induction next to the colonized tissue, but its expression
173 appeared to be limited to the outer tissues, the epidermis and cortex, rather than the colonized
174 vasculature (Fig. 3C, D). The strong induction of the *PEPs* and *PEPRs* remained visible for
175 roughly 10 to 12 cells, and then tapered out, eventually returning to the expression pattern of the
176 uninfected control.

177 Since it was shown that the ability of the PEPs and PEPRs to induce any signaling downstream of
178 the receptors is strictly dependent on the activity of the cytoplasmic kinase BIK1, we also
179 investigated the responsiveness of a *BIK1* (pGG-PIP22) transcriptional reporter (Liu *et al.*, 2013;
180 Yamada *et al.*, 2016). Under uninfected control conditions, *BIK1* is expressed in the MZ and DZ,
181 with stronger expression in the outer tissues, and only weak expression in the vascular tissue of
182 the MZ, somewhat resembling the expression pattern of *PEP2* (compare Fig. S3A-D and S1E-H).
183 Following colonization of the root by *Fo*5176, this pattern changed significantly, with *BIK1* now
184 expressed specifically in the cells immediately bordering the colonized tissue, with a clearly visible
185 expression maximum in the vasculature (Fig. 4A, B). Hence, the expression maxima of *BIK1*,
186 *PEP1*, *PEPR1* and *PEPR2* all overlapped in a small group of vascular cells closest to the colonized
187 tissue. *BIK1* however, also showed expression in the endodermis and cortex, albeit at a much lower
188 level than in the vasculature, while *PEP1* and *PEPRs* expression were restricted to the vasculature
189 (Fig. 3 and Fig. 4A, B).

190 One of the downstream outputs of PEP-activated BIK1 is the activation of the NADPH oxidase
191 RBOHD to trigger an apoplastic ROS-burst (Holmes *et al.*, 2018; Jing *et al.*, 2020). We therefore
192 investigated if *RBOHD* (pGG-PIP31) is also activated in the cells expressing *PEP1*, the *PEPRs*
193 and *BIK1*. Under uninfected control conditions, *RBOHD* is expressed in all cells and tissues of the
194 DZ, but not in the root tip (MZ, EZ) (Fig. S3E-H). Upon infection by *Fo*5176, expression is
195 activated in the cells next to the colonization site, even if they are still part of the EZ, which
196 normally does not express *RBOHD* (Fig. 4C, D). The pattern we observed very much resembled

bioRxiv preprint doi: https://doi.org/10.1101/2022.12.20.521163; this version posted April 18, 2023. The copyright holder for this preprint (which was not certified by peer review) is the author/funder, who has granted bioRxiv a license to display the preprint in perpetuity. It is made available under aCC-BY 4.0 International license.

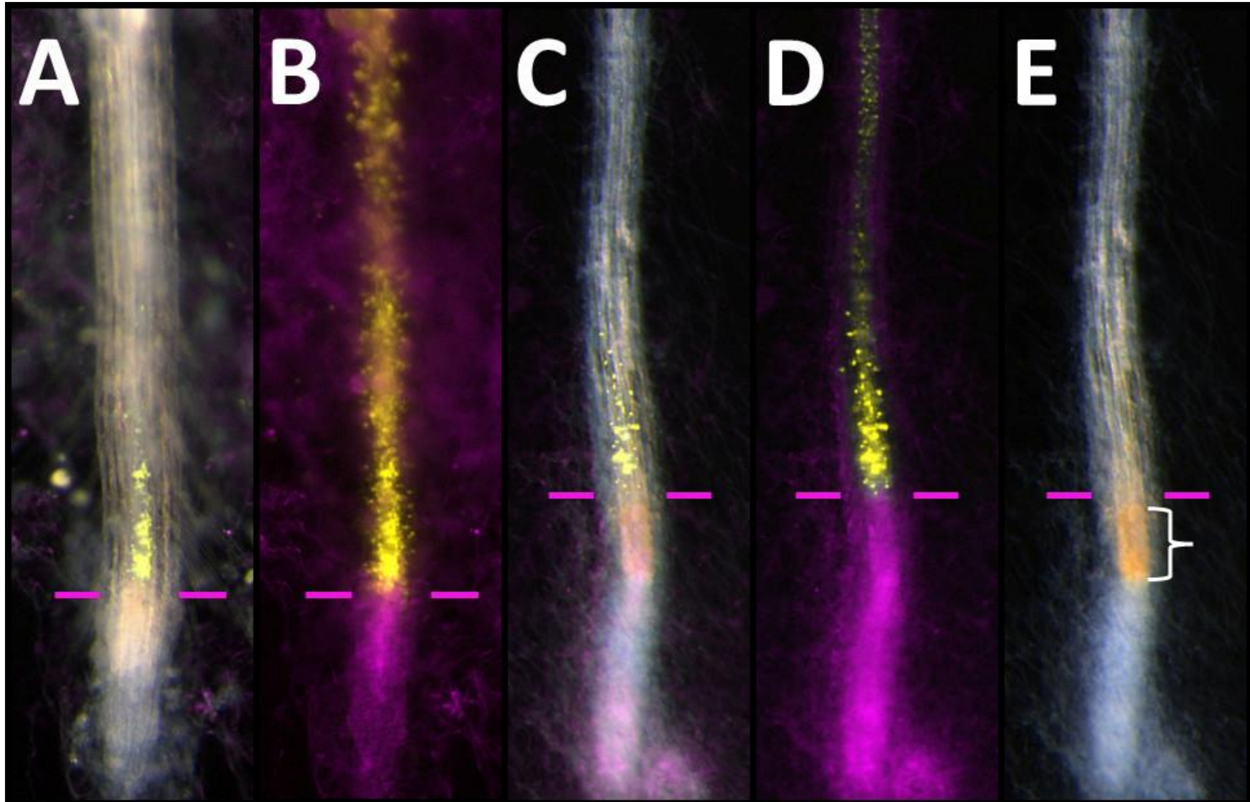

Figure 4: Transcriptional responses of *BIK1* and *RBOHD* expression to colonization by *Fo*5176
Bright field and fluorescence (**A, C**), fluorescence only (**B, D**), or bright field only (**E**) images of a colonized root expressing the *BIK1* (A, B), or *RBOHD* (C, D, E) reporters. The *Fo*5176 is shown in magenta, the reporters in yellow. The purple bars indicate the fungal colonization front. The white bracket in E indicates the area with 'root browning'.

197 the pattern of *BIK1* expression in response to colonization, with a maximum in a small group of
198 vascular cells next to the colonization site (Fig. 4). However, in contrast to the expression of *BIK1*
199 and the *PEPs* and *PEPRs*, upregulation of *RBOHD* appeared to be more spatially restricted to the
200 cells closest to the colonization site. *RBOHD* expression quickly returned to control levels behind
201 this small group of cells, while the activation of the other markers appeared to taper out more
202 gradually, across a longer stretch of cells.

203 While imaging the fungal infected reporter lines, we also regularly observed a discoloration of the
204 root in the colonized tissue (white bracket in Fig. 4E). This has previously been described as 'root
205 browning', and has been observed in response to infection by *F. oxysporum* or treatment of the
206 plant with SERINE-RICH ENDOGENOUS PEPTIDEs (Tintor *et al.*, 2020; Hou *et al.*, 2021).
207 While it remains unclear what the exact cause for this discoloration is, redox/oxidative stress
208 induced by ROS is one possibility. In our assay, the browning does not completely overlap with

bioRxiv preprint doi: https://doi.org/10.1101/2022.12.20.521163; this version posted April 18, 2023. The copyright holder for this preprint (which was not certified by peer review) is the author/funder, who has granted bioRxiv a license to display the preprint in perpetuity. It is made available under aCC-BY 4.0 International license.

209 the expression maximum of *RBOHD*, but as the colonization of the fungus progresses upward
210 through the vasculature, the *RBOHD* expression also extends along adjacent to the colonization
211 front. Therefore, the area showing root browning would be the region that last expressed *RBOHD*
212 at high levels, and thus could have been under redox/oxidative stress, but this requires further
213 examination.

214 **Discussion**

215 In this paper we present a GreenGate-based entry vector set with 75 plant immune system
216 promoters. In combination with the basic GreenGate kit from Lampropoulos et al. (2013) this is
217 already sufficient to build simple tools, such as transcriptional reporter lines, that can then be
218 probed for their responsiveness to a pathogen, elicitor, or other stimulant. Furthermore, owing to
219 the universal compatibility of these entry vectors with all other GreenGate-based systems, this
220 vector set can be used to screen for interactors of proteins in their native expression domain using
221 the proximity ligation kit from Goslin *et al.* (2021), or for tissue-specific gene knockouts by
222 combining them with the CRISPR-TSKO kit from Decaestecker *et al.* (2019), to name just two
223 possibilities.

224 As a straightforward proof-of-principle, we used some of the pGG-PIPs to create fluorescent
225 reporter lines for the PEP pathway and demonstrate how these can be used to gain insights into
226 *spatial immunity* – the highly localized activation of an immune pathway. Using these lines, we
227 showed that *PEP1*, and to some degree *PEP2*, were responsive to infection and colonization by
228 the vascular pathogen *Fo*5176. The danger signal PEP1 was upregulated in a specific group of
229 vascular cells immediately adjacent to the fungal colonization site, as were the two receptors
230 *PEPR1* and *2*. We thus hypothesize that activation of the PEP pathway is part of the plant's
231 immune response to infection and colonization by *Fo*5176. Importantly, we could show the highly
232 targeted activation of this pathway in just a couple of vascular cells immediately adjacent to a
233 colonization site. Such a local response has rarely been shown *in vivo* and *in planta* before, and is
234 typically overlooked in large-scale transcriptomic analyses.

235 Since the PEPRs are unlikely to serve as pattern-recognition receptors (PRRs) to sense the
236 pathogen, it is more likely that the PEPRs are part of a larger complex containing the PRR co-
237 receptor BAK1, as well as other PRRs, such as MIK2 or FER, since the interaction between BAK1

bioRxiv preprint doi: https://doi.org/10.1101/2022.12.20.521163; this version posted April 18, 2023. The copyright holder for this preprint (which was not certified by peer review) is the author/funder, who has granted bioRxiv a license to display the preprint in perpetuity. It is made available under aCC-BY 4.0 International license.

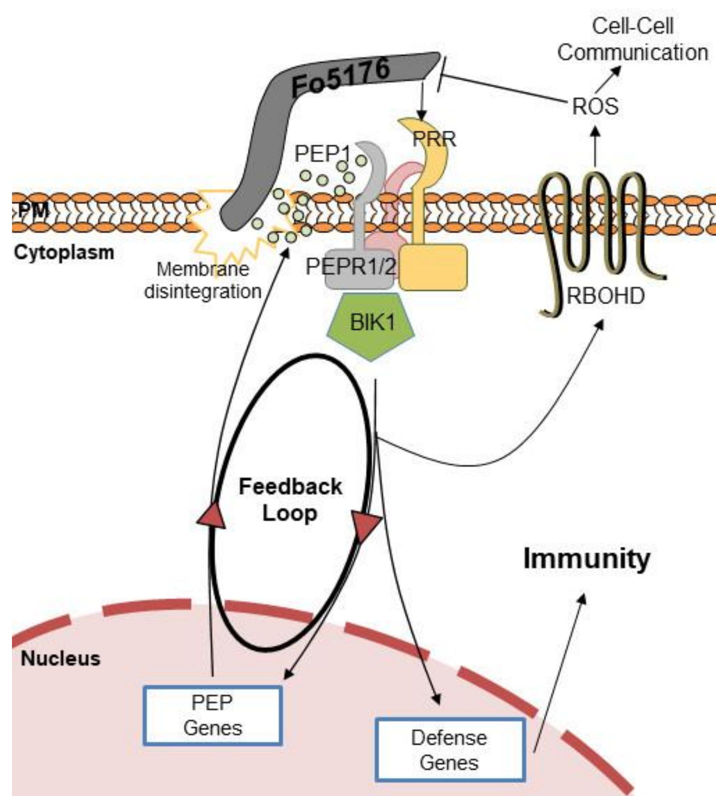

Figure 5: Model of the PEP pathway in response to *Fo*5176
Alkalinization of the apoplast via *Fo*5176-derived alkalinization factors induces interaction of the PEPRs with their PRR co-receptors. Intracellularly the receptors phosphorylate and activate BIK1. BIK1 activates expression of PEP1, thereby amplifying the PEP signal and creating a positive feedback loop. BIK1 also activates other defense genes, possibly via a MAPK cascade, and activates RBOHD to produce an apoplastic ROS-burst, which is damaging to the pathogen, and functions as cell-cell communication signal.

and the PEPRs has been previously shown, and all of these PRRs have been implicated to function in the defense against *Fo*5176 (Yamada *et al.*, 2016; Wang *et al.*, 2022*a*) (Fig. 5). Possibly,
243 these co-receptors are all co-localized in plasma membrane nanodomains to facilitate the rapid
244 assembly of larger receptor platforms (Somssich *et al.*, 2015; McKenna *et al.*, 2019; Somssich,
245 2020; Gronnier *et al.*, 2022). Indeed, rather than functioning as a PRR sensing the pathogen
246 directly, work from a recent publication suggests that the PEPRs act as extracellular pH sensors
247 (Liu *et al.*, 2022). Alkalinization of the apoplast is a hallmark of activated immunity, and Liu *et*
248 *al.*, (2022) show that the PEPRs specifically interact with their co-receptor BAK1 under alkaline
249 conditions, while they only show a weak affinity for interaction under acidic conditions (Felix *et*
250 *al.*, 1993; Liu *et al.*, 2022). Interestingly, *F. oxysporum* uses functional homologs of plant RAPID
251 ALKALINIZATION FACTORs to induce alkalinization of the apoplast, as this also stimulates
252 infectious growth of the fungus (Masachis *et al.*, 2016; Wang *et al.*, 2022*a*). Thus, the PEPRs
253 pathway may act as pH sensors to counteract this action by the fungus, improving the plant's
254 defense under these alkaline conditions. Extracellular binding of the PEPs to their receptors
255 generally leads to the activation of the PEPRs intracellular kinase domain and trans-
256 phosphorylation of the interacting cytoplasmic kinase BIK1 (Liu *et al.*, 2013). Indeed, we could
257 show that our *BIK1* reporter is also activated in the same pattern as the *PEP1* and the *PEPR*
258 reporters. BIK1 activation then facilitates downstream intracellular signaling (Yamada *et al.*,

bioRxiv preprint doi: https://doi.org/10.1101/2022.12.20.521163; this version posted April 18, 2023. The copyright holder for this preprint (which was not certified by peer review) is the author/funder, who has granted bioRxiv a license to display the preprint in perpetuity. It is made available under aCC-BY 4.0 International license.

259 2016). These downstream signaling events eventually result in the transcriptional activation of
260 defense genes, but also auto-activation of the *PEP* genes (Fig. 5). Since the PEPs do not have an
261 identifiable secretion signal that would direct them into the secretory pathway, it is assumed that
262 they are released into the apoplast indirectly when a pathogen breaches the plasma membrane and
263 causes local membrane disintegration (Fig. 5) (Yamaguchi and Huffaker, 2011; Yamada *et al.*,
264 2016). Once in the apoplast, they are then perceived by the PEPRs, creating a positive feedback-
265 loop of PEP-signaling and an auto-amplification of the plant's defense response (Fig. 5). A second
266 intracellular pathway activated via BIK1 leads to activation of the NADPH oxidase RBOHD (Fig.
267 5) (Kadota *et al.*, 2014; Holmes *et al.*, 2018; Jing *et al.*, 2020). This pathway was proposed to be
268 primarily driven by PEP1 and the PEPR2 (Jing *et al.*, 2020) and indeed, *PEP1* and *PEPR2* are also
269 the two reporters showing the strongest response to colonization by *Fo*5176, while *PEP2* was
270 primarily upregulated in the cells around the vasculature. *PEPR1* was also activated in the same
271 pattern as *PEP1*, *PEPR2*, and *BIK1*, but at a much lower level compared to *PEPR2*. Further, we
272 could also confirm that *RBOHD* expression is activated in these same cells, indicating that this
273 *BIK1*-*RBOHD*-dependent pathway for ROS-release is also potentially involved in the defense
274 against *Fo*5176 (Fig. 5). The activation of RBOHD, and the resulting ROS-burst, would aid in the
275 plant's defense against *Fo*5176, with ROS being directly harmful to the pathogen. Additionally,
276 ROS is known to also function as a signal in cell-cell communication to prime the surrounding
277 tissue for impeding attack (Waszczak *et al.*, 2018). We believe that the local 'root browning' that
278 we observed in the infected roots is likely the result of this apoplastic ROS-burst.

279 A role for the PEP-pathway in the defense against *F. oxysporum* has previously been hypothesized
280 on the basis of transcriptomic data showing up- or downregulation of some of the components in
281 response to infection (Fallath *et al.*, 2017; Guo *et al.*, 2021; Wang *et al.*, 2022*a*). By investigating
282 the responsiveness of our transcriptional reporters for PEP1 and 2, as well as PEPR1 and 2, we
283 added spatial resolution to the available transcriptomic data. We could show that PEP1 and the
284 PEPRs act in a clearly defined group of vascular cells immediately next to the fungal colonization
285 site, and this localized response overlaps with the activation of downstream signaling factors and
286 a local ROS-burst. *PEP2* was also induced in response to colonization, but it appeared to be
287 upregulated in the outer tissues, not the infected vasculature. While this may indicate a role for
288 PEP2 in priming these neighboring tissues, the fact that neither of the two *PEPRs* were expressed
289 there, makes it unclear how PEP2 would be perceived in these cells. Importantly, when Fallath *et*

bioRxiv preprint doi: https://doi.org/10.1101/2022.12.20.521163; this version posted April 18, 2023. The copyright holder for this preprint (which was not certified by peer review) is the author/funder, who has granted bioRxiv a license to display the preprint in perpetuity. It is made available under aCC-BY 4.0 International license.

290 *al.* (2017) investigated the transcriptional response of *med* mutants to infection by *Fo*5176, they
291 also only noted a deregulation of *PEP1* in these mutants, but not *PEP2*, indicating that *PEP1* is
292 indeed the major PEP signal acting in response to colonization by *Fo*5176.

293 Finally, we believe that the pGG-PIP plant immune promoter resource introduced in this article
294 will be valuable and helpful to the community for various research approaches. We will make the
295 75-plasmid collection available via AddGene for quick and simple distribution to the community.
296 We aim to provide further detailed 'spatial immunity' information by using these pGG-PIPs in our
297 future work.

298 Material & Methods

299 Cloning of the pGG-PIPs and transcriptional reporter constructs

300 The pGG-PIP entry vectors are based on the pGGA000 vector from the original GreenGate kit
301 (Lampropoulos *et al.*, 2013). The different promoters were amplified from total cellular *A. thaliana*
302 (natural accession Columbia) DNA, extracted from rosette leaves with the Qiagen DNeasy Plant
303 Kit, and using the primers in supplementary table 1. For error-free amplification, the Phusion high-
304 fidelity DNA polymerase with proofreading (New England Biolabs) was used. The fragments were
305 then transferred into pGGA000 in a Golden Gate assembly reaction using the NEBridge Golden
306 Gate Assembly Kit (BsaI-HF v2) (New England Biolabs). To clone the transcriptional reporter
307 lines, we used the destination vector pGGZ003, as well as the donor vectors pGGD007 (*linker-*
308 *NLS* (Nuclear Localization Signal)), pGGE009 (*UBQ10* terminator), and pGGF005
309 (*pUBQ10::HygR:tOCS*) from the original GreenGate kit from Lampropoulos *et al.* (2013). pGGB-
310 mT2 (*mTurquoise2*) and pGGC-mT2 (*mTurquoise2*) were created by cloning the *mT2* coding
311 sequence from an AddGene-derived template into pGGB000 and pGGC000 from the original
312 GreenGate kit (Goedhart *et al.*, 2012; Lampropoulos *et al.*, 2013). In combination with our pGG-
313 PIPs, this yielded the *pPIP::mT2-mT2-NLS:tUBQ10:pUBQ10::HygR:tOCS* reporters.

314 Plant growth and transformation

315 *A. thaliana* Columbia plants (Somssich, 2018) were grown at 16-hour light conditions, with 21 °C
316 during the light hours, and 18 °C during the dark hours. Light intensity was 120 mmol $m^{-2}s^{-1}$, and
317 humidity was 70%. Plant transformation was done via the *Agrobacterium tumefaciens* host strain
318 GV3101 *pMP90 pSoup* carrying one of the plasmids in table 1 using the floral dip method (Holsters
319 *et al.*, 1980; Koncz and Schell, 1986; Clough and Bent, 1998; Hellens *et al.*, 2000; Somssich,

bioRxiv preprint doi: https://doi.org/10.1101/2022.12.20.521163; this version posted April 18, 2023. The copyright holder for this preprint (which was not certified by peer review) is the author/funder, who has granted bioRxiv a license to display the preprint in perpetuity. It is made available under aCC-BY 4.0 International license.

320 2019). Individual resistant bacteria colonies were selected after two days of growth at 28° C on
321 YT plates (Miller, 1972) supplemented with 50 µg/ml rifampicin, 25 µg/ml gentamycin, 5 µg/ml
322 tetracyclin, and 100 µg/ml spectinomycin, then grown overnight in 250 ml of liquid 2×YT medium
323 with 50 µg/ml rifampicin, 25 µg/ml gentamycin, and 100 µg/ml spectinomycin, shaking at 200
324 rpm. Cells were harvested by centrifugation at 3200 *g* for 20 min, and resuspended in 300 ml of a
325 5% sucrose solution with 0.08% Silwet L-77. Plants were then dipped into the solution for
326 approximately 30 seconds with gentle agitation and laid out into a tray covered with cling wrap
327 overnight to maintain humidity. The next day they were returned to upright, and the procedure was
328 repeated after seven days. Once the siliques had ripened, the seeds were harvested and dried for at
329 least two weeks. For the selection of positive transformants, seeds were surface-sterilized using
330 75% ethanol with 0.1% Triton X-100 on a rotating incubator for at least two hours, after which the
331 seeds were decanted onto filter paper and the ethanol left to evaporate. Once the seeds were dry,
332 they were sprinkled onto a plate of half-strength basal Murashige & Skoog (MS) medium with
333 vitamins and 30 µg/ml hygromycin B, wrapped in aluminum foil, and stratified at 4 °C for three
334 days (Murashige and Skoog, 1962). They were then placed into a growth cabinet for 10 to 14 days,
335 after which healthy looking seedlings were transferred to half-strength MS plates without the
336 hygromycin, and grown for another two weeks, at which stage they were transferred to soil.

337 **Fungal growth and transformation**

338 The *F. oxysporum* f. sp. *conglutinans* strain 5176 was collected in 1971 from white cabbage
339 (*Brassica oleracea* var. *capitata* (L.)) in Australia (Wang *et al.*, 2022*a*). It has since been
340 maintained by the Brisbane Pathology (BRIP) Plant Pathology Herbarium in Queensland,
341 Australia under the accession number BRIP 5176 a. It was first used as a model pathogen for *A.*
342 *thaliana* by (Campbell *et al.*, 2003). To generate a *Fo*5176 line expressing cytoplasmic tdTomato
343 (tdT), an expression clone was generated by cloning the *tdT* coding sequence (amplified from an
344 AddGene-derived plasmid (Shaner *et al.*, 2004)) into the *Bgl*II cloning site of plasmid pLAU2
345 using Gibson assembly (Idnurm *et al.*, 2017). This places the gene under the control of a
346 constitutive promoter from the *actin* gene of ascomycete *Leptosphaeria maculans*. After
347 replication in *E. coli*, this plasmid pMAI32 was electroporated into *A. tumefaciens* strain EHA105
348 with selection on LB medium with kanamycin (50 µg/ml). *Fo*5176 was routinely cultured on
349 potato dextrose agar (PDA) plates. To generate spores for transformation, five plugs of about 5
350 mm diameter were inoculated into 50 ml half strength potato dextrose broth and cultured at 150

bioRxiv preprint doi: https://doi.org/10.1101/2022.12.20.521163; this version posted April 18, 2023. The copyright holder for this preprint (which was not certified by peer review) is the author/funder, who has granted bioRxiv a license to display the preprint in perpetuity. It is made available under aCC-BY 4.0 International license.

351 rpm for five days at room temperature, then filtered through miracloth, centrifuged at 3000 g for
352 5 min, and resuspended in sterile H_2O. The spores were then transformed with the *A. tumefaciens*
353 strain that had been cultured overnight in LB broth with kanamycin, using standard methods
354 (Idnurm *et al.*, 2017). That is, fungal spores and bacteria were mixed on induction medium plates
355 and cocultured for three days. Selection for transformants used an overlay of PDA supplemented
356 with hygromycin and cefotaxime (50 µg/ml and 100 µg/ml, respectively). Transformants that grew
357 through the overlaid medium, were subcultured onto PDA containing hygromycin and cefotaxime
358 and allowed to produce conidia, which were separated with a metal loop to generate strains derived
359 from a single conidium.

360 **Plant-fungus co-cultivation and infection**

361 To obtain fungal spores, *Fo*5176 was grown for at least seven days on PDA plates at room
362 temperature, at which time five pieces of roughly 1 mm^2 size were cut from the plate and dropped
363 into a flask containing 50 ml yeast nitrogen base (YNB) medium with 1% sucrose. The liquid
364 cultures were incubated for four days at room temperature with shaking at 120 rpm. The solution
365 was then filtered through miracloth, the spores harvested by centrifugation at 3000 rcf for 10 min
366 and resuspended in 25 ml sterile MilliQ water. For the co-cultivation of plant and fungus, *A.*
367 *thaliana* seedlings were grown on a vertical petri dish containing half-strength basal MS medium
368 with vitamins for 11 days and then transferred to a horizontal petri dish with a 2-3 cm strip of half-
369 strength basal MS medium with vitamins at the top end, while the rest of the plate was filled
370 roughly 2-3 mm high with liquid quarter-strength basal MS medium with vitamins (this is a setup
371 with slight modifications as described in (Tintor *et al.*, 2020)). The seedlings were placed onto the
372 thin MS medium strip at the top end, with the root in the liquid medium. Fungal spores were then
373 added to the liquid medium. The plates were covered with aluminum foil up until the leaves of the
374 plant, and then placed into a growth chamber.

375 **Microscopy**

376 We imaged the infection and the progression of colonization on a Leica M205 FA
377 stereomicroscope. Infection could usually be observed on day three after spored addition, and at
378 day 5 there was robust colonization. We usually imaged daily from day 3 to 11 dpi. For the
379 fluorescence coming from the plant 2xmT2 reporters, we used the Leica ET CFP (ET436/20x
380 ET480/40m) filter, and for the fungal tdT reporter the Leica ET mCHER (ET560/40x ET630/75m)

bioRxiv preprint doi: https://doi.org/10.1101/2022.12.20.521163; this version posted April 18, 2023. The copyright holder for this preprint (which was not certified by peer review) is the author/funder, who has granted bioRxiv a license to display the preprint in perpetuity. It is made available under aCC-BY 4.0 International license.

381 filter. We use 80× magnification for the images used in this paper. The settings for the imaging
382 (illumination strength, exposure time, gain, etc.) were kept constant for all imaging sessions, to
383 allow for at least semi-quantitative imaging, and to make the images at least relatively comparable.
384 The images were recorded using the Leica Application Suite software, and processed using Fiji Is
385 Just ImageJ (FIJI) and the GNU Image Manipulation Program (GIMP) (Schindelin *et al.*, 2012).

386 **Data availability**

387 We have donated the pGG-PIP vector collection to AddGene (Deposit-ID: 82532, Catalog-#:
388 196739-196813).

389 **Acknowledgements**

390 This work was funded by the Australian Research Council (grant no. DE200101560) and was
391 further supported by a seed grant from the Melbourne University Botany Foundation. LW was
392 supported by the China Scholarship Council. H-WC was supported by a Graduate Research
393 Scholarship from the University of Melbourne. Imaging was done on instruments maintained by
394 the Biological Optical Microscopy Platform (BOMP) and the BioSciences Microscopy Unit at the
395 University of Melbourne. The authors would like to thank Dr. Imre E. Somssich for critical reading
396 of the manuscript.

397 **References**

398 **Acevedo-Garcia J, Gruner K, Reinstädler A, *et al.*** 2017. The powdery mildew-resistant
399 Arabidopsis mlo2 mlo6 mlo12 triple mutant displays altered infection phenotypes with diverse
400 types of phytopathogens. Scientific reports **7**, 9319.

401 **Andersen TG, Barberon M, Geldner N**. 2015. Suberization-the second life of an endodermal
402 cell. Current Opinion in Plant Biology **28**, 9–15.

403 **Bird JE, Marles-Wright J, Giachino A**. 2022. A User's Guide to Golden Gate Cloning
404 Methods and Standards. ACS Synthetic Biology.

405 **Birkenbihl RP, Kracher B, Ross A, Kramer K, Finkemeier I, Somssich IE**. 2018. Principles
406 and characteristics of the Arabidopsis WRKY regulatory network during early MAMP-triggered
407 immunity. The Plant Journal.

bioRxiv preprint doi: https://doi.org/10.1101/2022.12.20.521163; this version posted April 18, 2023. The copyright holder for this preprint (which was not certified by peer review) is the author/funder, who has granted bioRxiv a license to display the preprint in perpetuity. It is made available under aCC-BY 4.0 International license.

408 **Birkenbihl RP, Kracher B, Somssich IE**. 2017*a*. Induced Genome-Wide Binding of Three
409 Arabidopsis WRKY Transcription Factors during Early MAMP-Triggered Immunity. The Plant
410 cell **29**, 20–38.

411 **Birkenbihl RP, Liu S, Somssich IE**. 2017*b*. Transcriptional events defining plant immune
412 responses. Current Opinion in Plant Biology **38**, 1–9.

413 **Blümke A, Somerville SC, Voigt CA**. 2013. Transient expression of the Arabidopsis thaliana
414 callose synthase PMR4 increases penetration resistance to powdery mildew in barley. Advances
415 in Bioscience and Biotechnology **04**, 810–813.

416 **Cai Q, Qiao L, Wang M, He B, Lin F, Palmquist J, Huang S-D, Jin H**. 2018. Plants send
417 small RNAs in extracellular vesicles to fungal pathogen to silence virulence genes. Science **360**,
418 1126–1129.

419 **Calabria J, Wang L, Rast-Somssich MI, Chen H-W, Watt M, Persson S, Idnurm A,**
420 **Somssich M**. 2022. Spatially distinct phytohormone responses of individual Arabidopsis thaliana
421 root cells to infection and colonization by Fusarium oxysporum. bioRxiv, 521292.

422 **Campbell EJ, Schenk PM, Kazan K, Penninckx IAMA, Anderson JP, Maclean DJ,**
423 **Cammue BPA, Ebert PR, Manners JM**. 2003. Pathogen-responsive expression of a putative
424 ATP-binding cassette transporter gene conferring resistance to the diterpenoid sclareol is
425 regulated by multiple defense signaling pathways in Arabidopsis. Plant physiology **133**, 1272–
426 84.

427 **Cao Y, Liang Y, Tanaka K, Nguyen CT, Jedrzejczak RP, Joachimiak A, Stacey G**. 2014.
428 The kinase LYK5 is a major chitin receptor in Arabidopsis and forms a chitin-induced complex
429 with related kinase CERK1. eLife **3**, 1–19.

430 **Cho H, Lee J, Oh E**. 2022. Leucine-Rich Repeat Receptor-Like Proteins in Plants: Structure,
431 Function, and Signaling. Journal of Plant Biology.

432 **Chuberre C, Plancot B, Driouich A, Moore JP, Bardor M, Gügi B, Vicré M**. 2018. Plant
433 Immunity Is Compartmentalized and Specialized in Roots. Frontiers in Plant Science **9**, 1–13.

434 **Clough SJ, Bent AF**. 1998. Floral dip: a simplified method for Agrobacterium-mediated
435 transformation of Arabidopsis thaliana. The Plant Journal **16**, 735–43.

bioRxiv preprint doi: https://doi.org/10.1101/2022.12.20.521163; this version posted April 18, 2023. The copyright holder for this preprint (which was not certified by peer review) is the author/funder, who has granted bioRxiv a license to display the preprint in perpetuity. It is made available under aCC-BY 4.0 International license.

436 **Couto D, Zipfel C**. 2016. Regulation of pattern recognition receptor signalling in plants. Nature
437 reviews. Immunology **16**, 537–552.

438 **Decaestecker W, Buono RA, Pfeiffer ML, Vangheluwe N, Jourquin J, Karimi M, Van**
439 **Isterdael G, Beeckman T, Nowack MK, Jacobs TB**. 2019. CRISPR-TSKO: A Technique for
440 Efficient Mutagenesis in Specific Cell Types, Tissues, or Organs in Arabidopsis. The Plant Cell
441 **31**, 2868–2887.

442 **Denay G, Blümke P, Hänsch S, Weidtkamp-Peters S, Simon R**. 2019. Over the rainbow: A
443 practical guide for fluorescent protein selection in plant FRET experiments. Plant Direct **3**,
444 e00189.

445 **Dogra V, Singh RM, Li M, Li M, Singh S, Kim C**. 2022. EXECUTER2 modulates the
446 EXECUTER1 signalosome through its singlet oxygen-dependent oxidation. Molecular Plant **15**,
447 438–453.

448 **Duan Z, Liu W, Li K, Duan W, Zhu S, Xing J, Chen T, Luo X**. 2022. Regulation of immune
449 complex formation and signalling by FERONIA, a busy goddess in plant–microbe interactions.
450 Molecular Plant Pathology, 1–6.

451 **Engler C, Gruetzner R, Kandzia R, Marillonnet S**. 2009. Golden Gate Shuffling: A One-Pot
452 DNA Shuffling Method Based on Type IIs Restriction Enzymes (J Peccoud, Ed.). PLOS ONE **4**,
453 e5553.

454 **Engler C, Kandzia R, Marillonnet S**. 2008. A One Pot, One Step, Precision Cloning Method
455 with High Throughput Capability (HA El-Shemy, Ed.). PLOS ONE **3**, e3647.

456 **Fallath T, Kidd BN, Stiller J, Davoine C, Björklund S, Manners JM, Kazan K, Schenk PM**.
457 2017. MEDIATOR18 and MEDIATOR20 confer susceptibility to Fusarium oxysporum in
458 Arabidopsis thaliana. PLOS ONE **12**, e0176022.

459 **Felix G, Regenass M, Boller T**. 1993. Specific perception of subnanomolar concentrations of
460 chitin fragments by tomato cells: induction of extracellular alkalinization, changes in protein
461 phosphorylation, and establishment of a refractory state. The Plant Journal **4**, 307–316.

462 **Gao X, He P**. 2013. Nuclear dynamics of Arabidopsis calcium-dependent protein kinases in
463 effector-triggered immunity. Plant signaling & behavior **8**, e23868.

bioRxiv preprint doi: https://doi.org/10.1101/2022.12.20.521163; this version posted April 18, 2023. The copyright holder for this preprint (which was not certified by peer review) is the author/funder, who has granted bioRxiv a license to display the preprint in perpetuity. It is made available under aCC-BY 4.0 International license.

464 **Goedhart J, von Stetten D, Noirclerc-Savoye M, Lelimousin M, Joosen L, Hink MA, van**
465 **Weeren L, Gadella Jr. TWJ, Royant A**. 2012. Structure-guided evolution of cyan fluorescent
466 proteins towards a quantum yield of 93%. Nature communications **3**, 751.

467 **Gonçalves Dias M, Soleimani F, Monaghan J**. 2022. Activation and turnover of the plant
468 immune signaling kinase BIK1: a fine balance. Essays in Biochemistry, 1–12.

469 **Goslin K, Finocchio A, Wellmer F**. 2021. A Golden Gate-based Plasmid Library for the Rapid
470 Assembly of Biotin Ligase Constructs for Proximity Labelling. bioRxiv, 464533.

471 **Greenwood JR, Williams SJ**. 2022. Guarding the central regulator of extracellular perception in
472 plants – A job for two. Cell Host & Microbe **30**, 1657–1659.

473 **Gronnier J, Franck CM, Stegmann M, *et al.*** 2022. Regulation of immune receptor kinase
474 plasma membrane nanoscale organization by a plant peptide hormone and its receptors. eLife **11**,
475 212233.

476 **Guo L, Yu H, Wang B, *et al.*** 2021. Metatranscriptomic Comparison of Endophytic and
477 Pathogenic Fusarium –Arabidopsis Interactions Reveals Plant Transcriptional Plasticity.
478 Molecular Plant-Microbe Interactions **34**, 1071–1083.

479 **Hartley JL, Temple GF, Brasch MA**. 2000. DNA Cloning Using In Vitro Site-Specific
480 Recombination. Genome Research **10**, 1788–1795.

481 **Hellens RP, Edwards EA, Leyland NR, Bean S, Mullineaux PM**. 2000. pGreen: a versatile
482 and flexible binary Ti vector for Agrobacterium-mediated plant transformation. Plant molecular
483 biology **42**, 819–32.

484 **Holmes DR, Grubb LE, Monaghan J**. 2018. The jasmonate receptor COI1 is required for
485 AtPep1-induced immune responses in Arabidopsis thaliana. BMC Research Notes **11**, 555.

486 **Holsters M, Silva B, van Vliet F, *et al.*** 1980. The functional organization of the nopaline A.
487 tumefaciens plasmid pTiC58. Plasmid **3**, 212–230.

488 **Hou S, Liu D, Huang S, *et al.*** 2021. The Arabidopsis MIK2 receptor elicits immunity by
489 sensing a conserved signature from phytocytokines and microbes. Nature Communications **12**,
490 5494.

bioRxiv preprint doi: https://doi.org/10.1101/2022.12.20.521163; this version posted April 18, 2023. The copyright holder for this preprint (which was not certified by peer review) is the author/funder, who has granted bioRxiv a license to display the preprint in perpetuity. It is made available under aCC-BY 4.0 International license.

491 **Huerta AI, Sancho-Andrés G, Montesinos JC, *et al.*** 2023. The WAK-like protein RFO1 acts
492 as a sensor of the pectin methylation status in Arabidopsis cell walls to modulate root growth and
493 defense. Molecular Plant **2**, 33–47.

494 **Idnurm A, Urquhart AS, Vummadi DR, Chang S, Van de Wouw AP, López-Ruiz FJ**. 2017.
495 Spontaneous and CRISPR/Cas9-induced mutation of the osmosensor histidine kinase of the
496 canola pathogen Leptosphaeria maculans. Fungal Biology and Biotechnology **4**, 12.

497 **Jia A, Huang S, Song W, *et al.*** 2022. TIR-catalyzed ADP-ribosylation reactions produce
498 signaling molecules for plant immunity. Science **377**.

499 **Jin T, Wu H, Deng Z, Cai T, Li J, Liu Z, Waterhouse PM, White RG, Liang D**. 2022.
500 Control of root-to-shoot long-distance flow by a key ROS-regulating factor in Arabidopsis.
501 Plant, Cell & Environment, 0–2.

502 **Jing Y, Shen N, Zheng X, Fu A, Zhao F, Lan W, Luan S**. 2020. Danger-Associated Peptide
503 Regulates Root Immune Responses and Root Growth by Affecting ROS Formation in
504 Arabidopsis. International Journal of Molecular Sciences **21**, 4590.

505 **Joglekar S, Suliman M, Bartsch M, Halder V, Maintz J, Bautor J, Zeier J, Parker JE,**
506 **Kombrink E**. 2018. Chemical Activation of EDS1/PAD4 Signaling Leading to Pathogen
507 Resistance in Arabidopsis. Plant & Cell Physiology **59**, 1592–1607.

508 **Journot-Catalino N, Somssich IE, Roby D, Kroj T**. 2006. The transcription factors WRKY11
509 and WRKY17 act as negative regulators of basal resistance in Arabidopsis thaliana. The Plant
510 cell **18**, 3289–3302.

511 **Kadota Y, Sklenar J, Derbyshire P, *et al.*** 2014. Direct regulation of the NADPH oxidase
512 RBOHD by the PRR-associated kinase BIK1 during plant immunity. Molecular cell **54**, 43–55.

513 **Kaiser S, Eisa A, Kleine-Vehn J, Scheuring D**. 2019. NET4 Modulates the Compactness of
514 Vacuoles in Arabidopsis thaliana. International Journal of Molecular Sciences **20**, 4752.

515 **Kim SH, Lam PY, Lee M-H, Jeon HS, Tobimatsu Y, Park OK**. 2020. The Arabidopsis R2R3
516 MYB Transcription Factor MYB15 Is a Key Regulator of Lignin Biosynthesis in Effector-
517 Triggered Immunity. Frontiers in Plant Science **11**, 1–10.

bioRxiv preprint doi: https://doi.org/10.1101/2022.12.20.521163; this version posted April 18, 2023. The copyright holder for this preprint (which was not certified by peer review) is the author/funder, who has granted bioRxiv a license to display the preprint in perpetuity. It is made available under aCC-BY 4.0 International license.

518 **Koncz C, Schell J**. 1986. The promoter of TL-DNA gene 5 controls the tissue-specific
519 expression of chimaeric genes carried by a novel type of Agrobacterium binary vector.
520 Molecular & General Genetics **204**, 383–396.

521 **Kümpers BMC, Han J, Vaughan-Hirsch J, *et al.*** 2022. Dual expression and anatomy lines
522 allow simultaneous visualization of gene expression and anatomy. Plant Physiology **188**, 56–69.

523 **Lampropoulos A, Sutikovic Z, Wenzl C, Maegele I, Lohmann JU, Forner J**. 2013.
524 GreenGate - a novel, versatile, and efficient cloning system for plant transgenesis. PLOS ONE **8**,
525 e83043.

526 **Lee D-K, Parrott DL, Adhikari E, Fraser N, Sieburth LE**. 2016. The Mobile bypass Signal
527 Arrests Shoot Growth by Disrupting Shoot Apical Meristem Maintenance, Cytokinin Signaling,
528 and WUS Transcription Factor Expression. Plant Physiology **171**, 2178–2190.

529 **Liu J, Liu B, Chen S, *et al.*** 2018. A Tyrosine Phosphorylation Cycle Regulates Fungal
530 Activation of a Plant Receptor Ser/Thr Kinase. Cell Host & Microbe **23**, 241-253.e6.

531 **Liu L, Song W, Huang S, *et al.*** 2022. Extracellular pH sensing by plant cell-surface peptide-
532 receptor complexes. Cell, 1–15.

533 **Liu W, Wang C, Wang G, Ma Y, Tian J, Yu Y, Dong L, Kong Z**. 2019. Towards a better
534 recording of microtubule cytoskeletal spatial organization and dynamics in plant cells. Journal of
535 Integrative Plant Biology **61**, 388–393.

536 **Liu Z, Wu Y, Yang F, Zhang Y, Chen S, Xie Q, Tian X, Zhou J-M**. 2013. BIK1 interacts
537 with PEPRs to mediate ethylene-induced immunity. Proceedings of the National Academy of
538 Sciences of the United States of America **110**, 6205–6210.

539 **Long Y, Stahl Y, Weidtkamp-Peters S, Smet W, Du Y, Gadella Jr. TWJ, Goedhart J,**
540 **Scheres B, Blilou I**. 2018. Optimizing FRET-FLIM Labeling Conditions to Detect Nuclear
541 Protein Interactions at Native Expression Levels in Living Arabidopsis Roots. Frontiers in Plant
542 Science **9**, 1–13.

543 **Masachis S, Segorbe D, Turrà D, *et al.*** 2016. A fungal pathogen secretes plant alkalinizing
544 peptides to increase infection. Nature Microbiology **1**, 16043.

bioRxiv preprint doi: https://doi.org/10.1101/2022.12.20.521163; this version posted April 18, 2023. The copyright holder for this preprint (which was not certified by peer review) is the author/funder, who has granted bioRxiv a license to display the preprint in perpetuity. It is made available under aCC-BY 4.0 International license.

545 **McKenna JF, Rolfe DJ, Webb SED, Tolmie AF, Botchway SW, Martin-Fernandez ML,**
546 **Hawes C, Runions J**. 2019. The cell wall regulates dynamics and size of plasma-membrane
547 nanodomains in Arabidopsis. Proceedings of the National Academy of Sciences of the United
548 States of America, 201819077.

549 **Meng F, Ellis T**. 2020. The second decade of synthetic biology: 2010–2020. Nature
550 Communications **11**, 5174.

551 **Miller JH**. 1972. Formulas and recipes. Experiments in molecular genetics. Cold Spring Harbor,
552 New York: Cold Spring Harbor Laboratory, 433.

553 **Morales J, Kadota Y, Zipfel C, Molina A, Torres MÁ**. 2016. The Arabidopsis NADPH
554 oxidases RbohD and RbohF display differential expression patterns and contributions during
555 plant immunity. Journal of experimental botany **67**, 1663–76.

556 **Murashige T, Skoog F**. 1962. A Revised Medium for Rapid Growth and Bio Assays with
557 Tobaoco Tissue Cultures. Physiologia Plantarum **15**, 473–497.

558 **Ngou BPM, Ahn H, Ding P, Jones JDG**. 2021. Mutual potentiation of plant immunity by cell-
559 surface and intracellular receptors. Nature **592**, 110–115.

560 **Patil M, Senthil-Kumar M**. 2020. Role of Plant Kinases in Combined Stress. Protein Kinases
561 and Stress Signaling in Plants. Wiley, 445–458.

562 **Petutschnig E, Anders J, Stolze M, *et al.*** 2022. EXTRA LARGE G-PROTEIN2 mediates cell
563 death and hyperimmunity in the chitin elicitor receptor kinase 1-4 mutant. Plant Physiology **5**.

564 **Rhodes J, Yang H, Moussu S, Boutrot F, Santiago J, Zipfel C**. 2021. Perception of a
565 divergent family of phytocytokines by the Arabidopsis receptor kinase MIK2. Nature
566 Communications **12**, 705.

567 **Saijo Y, Loo EP, Yasuda S**. 2018. Pattern recognition receptors and signaling in plant-microbe
568 interactions. The Plant Journal **93**, 592–613.

569 **Salguero-Linares J, Serrano I, Ruiz-Solani N, Salas-Gómez M, Phukan UJ, González VM,**
570 **Bernardo-Faura M, Valls M, Rengel D, Coll NS**. 2022. Robust transcriptional indicators of
571 immune cell death revealed by spatiotemporal transcriptome analyses. Molecular Plant **15**,

bioRxiv preprint doi: https://doi.org/10.1101/2022.12.20.521163; this version posted April 18, 2023. The copyright holder for this preprint (which was not certified by peer review) is the author/funder, who has granted bioRxiv a license to display the preprint in perpetuity. It is made available under aCC-BY 4.0 International license.

572 1059–1075.

573 **Schindelin J, Arganda-Carreras I, Frise E, *et al.*** 2012. Fiji: an open-source platform for
574 biological-image analysis. Nature methods **9**, 676–82.

575 **Schürholz A-K, Lopez-Salmeron V, Li Z, *et al.*** 2018. A Comprehensive Toolkit for Inducible,
576 Cell Type-Specific Gene Expression in Arabidopsis. Plant Physiology, pp.00463.2018.

577 **Shaner NC, Campbell RE, Steinbach PA, Giepmans BNG, Palmer AE, Tsien RY**. 2004.
578 Improved monomeric red, orange and yellow fluorescent proteins derived from Discosoma sp.
579 red fluorescent protein. Nature biotechnology **22**, 1567–72.

580 **Somssich M**. 2018. A short history of Arabidopsis thaliana (L.) Heynh. Columbia-0. PeerJ
581 Preprints **e26931v3**, 1–7.

582 **Somssich M**. 2019. A short history of plant transformation. PeerJ Preprints, 1–28.

583 **Somssich M**. 2020. FERONIA is the new BAK1, and membrane nanodomains are the new thing
584 - but the flg22/FLS2/BAK1 complex continues to serve as a platform for new discoveries.
585 preLights, 23746.

586 **Somssich M**. 2022. The Dawn of Plant Molecular Biology: How Three Key Methodologies
587 Paved the Way. Current Protocols **2**, 1–19.

588 **Somssich M, Ma Q, Weidtkamp-Peters S, Stahl Y, Felekyan S, Bleckmann A, Seidel CAM,**
589 **Simon R**. 2015. Real-time dynamics of peptide ligand-dependent receptor complex formation in
590 planta. Science Signaling **8**, 1–9.

591 **Stegmann M, Monaghan J, Smakowska-Luzan E, Rovenich H, Lehner A, Holton NJ,**
592 **Belkhadir Y, Zipfel C**. 2017. The receptor kinase FER is a RALF-regulated scaffold controlling
593 plant immune signaling. Science **355**, 287–289.

594 **Sun T, Zhang Y**. 2021. Short- and long-distance signaling in plant defense. The Plant Journal
595 **105**, 505–517.

596 **Tanaka T, Ikeda A, Shiojiri K, *et al.*** 2018. Identification of a Hexenal Reductase That
597 Modulates the Composition of Green Leaf Volatiles. Plant Physiology **178**, 552–564.

598 **Tintor N, Paauw M, Rep M, Takken FLW**. 2020. The root-invading pathogen Fusarium

bioRxiv preprint doi: https://doi.org/10.1101/2022.12.20.521163; this version posted April 18, 2023. The copyright holder for this preprint (which was not certified by peer review) is the author/funder, who has granted bioRxiv a license to display the preprint in perpetuity. It is made available under aCC-BY 4.0 International license.

599 oxysporum targets pattern-triggered immunity using both cytoplasmic and apoplastic effectors.
600 New Phytologist **227**, 1479–1492.

601 **Tseng Y, Scholz SS, Fliegmann J, Krüger T, Gandhi A, Furch ACU, Kniemeyer O,**
602 **Brakhage AA, Oelmüller R**. 2022. CORK1, A LRR-Malectin Receptor Kinase, Is Required for
603 Cellooligomer-Induced Responses in Arabidopsis thaliana. Cells **11**, 2960.

604 **Tsuda K, Somssich IE**. 2015. Transcriptional networks in plant immunity. New phytologist
605 **206**, 932–47.

606 **Wang L, Calabria J, Chen H-W, Somssich M**. 2022*a*. The Arabidopsis thaliana – Fusarium
607 oxysporum strain 5176 pathosystem: an overview (M Höfte, Ed.). Journal of Experimental
608 Botany, erac263.

609 **Wang W, Liu J, Mishra B, Mukhtar MS, McDowell JM**. 2022*b*. Sparking a sulfur war
610 between plants and pathogens. Trends in Plant Science, 1–13.

611 **Wang X, Meng H, Tang Y, Zhang Y, He Y, Zhou J, Meng X**. 2022*c*. Phosphorylation of an
612 ethylene response factor by MPK3/MPK6 mediates negative feedback regulation of pathogen-
613 induced ethylene biosynthesis in Arabidopsis. Journal of Genetics and Genomics **49**, 810–822.

614 **Wang J, Zhang Y, Wu J, Meng L, Ren H**. 2013. AtFH16, an Arabidopsis type II formin, binds
615 and bundles both microfilaments and microtubules, and preferentially binds to microtubules.
616 Journal of integrative plant biology **55**, 1002–15.

617 **Waszczak C, Carmody M, Kangasjärvi J**. 2018. Reactive Oxygen Species in Plant Signaling.
618 Annual Review of Plant Biology **69**, 209–236.

619 **Weber E, Engler C, Gruetzner R, Werner S, Marillonnet S**. 2011. A Modular Cloning
620 System for Standardized Assembly of Multigene Constructs (J Peccoud, Ed.). PLOS ONE **6**,
621 e16765.

622 **Wirthmueller L, Zhang Y, Jones JDG, Parker JE**. 2007. Nuclear Accumulation of the
623 Arabidopsis Immune Receptor RPS4 Is Necessary for Triggering EDS1-Dependent Defense.
624 Current Biology **17**, 2023–2029.

625 **Wu J, Liu Z, Zhang Z, *et al.*** 2016. Transcriptional regulation of receptor-like protein genes by

bioRxiv preprint doi: https://doi.org/10.1101/2022.12.20.521163; this version posted April 18, 2023. The copyright holder for this preprint (which was not certified by peer review) is the author/funder, who has granted bioRxiv a license to display the preprint in perpetuity. It is made available under aCC-BY 4.0 International license.

626 environmental stresses and hormones and their overexpression activities in Arabidopsis thaliana.
627 Journal of Experimental Botany **67**, 3339–3351.

628 **Wu R, Lucke M, Jang Y, Zhu W, Symeonidi E, Wang C, Fitz J, Xi W, Schwab R, Weigel**
629 **D**. 2018. An efficient CRISPR vector toolbox for engineering large deletions in Arabidopsis
630 thaliana. Plant Methods **14**, 65.

631 **Yamada K, Yamashita-Yamada M, Hirase T, Fujiwara T, Tsuda K, Hiruma K, Saijo Y**.
632 2016. Danger peptide receptor signaling in plants ensures basal immunity upon pathogen-
633 induced depletion of BAK1. The EMBO journal **35**, 46–61.

634 **Yamaguchi Y, Huffaker A**. 2011. Endogenous peptide elicitors in higher plants. Current
635 Opinion in Plant Biology **14**, 351–357.

636 **Yamaguchi Y, Huffaker A, Bryan AC, Tax FE, Ryan CA**. 2010. PEPR2 Is a Second Receptor
637 for the Pep1 and Pep2 Peptides and Contributes to Defense Responses in Arabidopsis. The Plant
638 Cell **22**, 508–522.

639 **Yamaguchi Y, Pearce G, Ryan CA**. 2006. The cell surface leucine-rich repeat receptor for
640 AtPep1, an endogenous peptide elicitor in Arabidopsis, is functional in transgenic tobacco cells.
641 Proceedings of the National Academy of Sciences of the United States of America **103**, 10104–9.

642 **Yang W, Devaiah SP, Pan X, Isaac G, Welti R, Wang X**. 2007. AtPLAI Is an Acyl Hydrolase
643 Involved in Basal Jasmonic Acid Production and Arabidopsis Resistance to Botrytis cinerea.
644 Journal of Biological Chemistry **282**, 18116–18128.

645 **Yang J, Duan G, Li C, Liu L, Han G, Zhang Y, Wang C**. 2019. The Crosstalks Between
646 Jasmonic Acid and Other Plant Hormone Signaling Highlight the Involvement of Jasmonic Acid
647 as a Core Component in Plant Response to Biotic and Abiotic Stresses. Frontiers in Plant Science
648 **10**, 1–12.

649 **Yang F, Kimberlin AN, Elowsky CG, Liu Y, Gonzalez-Solis A, Cahoon EB, Alfano JR**.
650 2018. A Plant Immune Receptor Degraded by Selective Autophagy. Molecular Plant, 1–39.

651 **Zipfel C, Oldroyd GED**. 2017. Plant signalling in symbiosis and immunity. Nature **543**, 328–
652 336.

bioRxiv preprint doi: https://doi.org/10.1101/2022.12.20.521163; this version posted April 18, 2023. The copyright holder for this preprint (which was not certified by peer review) is the author/funder, who has granted bioRxiv a license to display the preprint in perpetuity. It is made available under aCC-BY 4.0 International license.

653

654

bioRxiv preprint doi: https://doi.org/10.1101/2022.12.20.521163; this version posted April 18, 2023. The copyright holder for this preprint (which was not certified by peer review) is the author/funder, who has granted bioRxiv a license to display the preprint in perpetuity. It is made available under aCC-BY 4.0 International license.

655 **Supplementary information:**

656 **Supplementary table 1: List of primers used to clone the promoters**

657 MAS-GG-ACS2p-F AACAGGTCTCAACCTCGGTCGATGTAAATGGATTAAATTTTATA
658 MAS-GG-ACS2p-R AACAGGTCTCATGTTGCTGTGTCAATTCTCACTTCTTTG
659 MAS-GG-ACS2pm-F AACAGGTCTCAGGTGTCCTCAAGGTTTCTGTTTCAAC
660 MAS-GG-ACS2pm-R AACAGGTCTCACACCAAATAAAGTTGATGTGGGGTC
661 MAS-GG-AOSp-F AACAGGTCTCAACCTACACTTAGACACCCCAATATTTTAGATTT
662 MAS-GG-AOSp-R AACAGGTCTCATGTTCTATTCGAAACAGTGGCGAGT
663 MAS-GG-AOSpm1-F AACAGGTCTCAGCCAATATTTTAGATTTTACTTTAAAGAAAT
664 MAS-GG-AOSpm1-R AACAGGTCTCATGGCGTCTCTAAGTGTTTTTTTTT
665 MAS-GG-AOSpm2-F AACAGGTCTCAGACACCTAAGTATTTTCTTTCCAACAA
666 MAS-GG-AOSpm2-R AACAGGTCTCATGTCCTTCTCTTTGAATAAACCTCA
667 MAS-GG-ARR5p-F AACAGGTCTCAACCTATATGATTTTTTCAAAAGAAAACACCATTTAGT
668 MAS-GG-ARR5p-R AACAGGTCTCATGTTATCAAGAAGAGTAGGATCGTGACTCGT
669 MAS-GG-ARR5pm-F AACAGGTCTCAGATTAGGATTATTCTTTATAGAATGTTTTGGTGC
670 MAS-GG-ARR5pm-R AACAGGTCTCAAATCGTCTCGGTTTTTACCTCTCAAATAGTAT
671 MAS-GG-ATG8Ap-F AACAGGTCTCAACCTTTAGCAGTGCTTAGTGAGCTTAAATTATAGTT
672 MAS-GG-ATG8Ap-R AACAGGTCTCATGTTAATTAATAAACTCGATCGTCTGCTAGATCG
673 MAS-GG-BAK1p-F AACAGGTCTCAACCTGTTTTTTGGAAACAGAGAGAAAACTCA
674 MAS-GG-BAK1p-R AACAGGTCTCATGTTTATCCTCAAGAGATTAAAAACAAACCCTA
675 MAS-GG-BIK1p-F AACAGGTCTCAACCTCGTTCCCAAATCTCGGTCAATTG
676 MAS-GG-BIK1p-R AACAGGTCTCATGTTCAAAGCTAAGAACAGATTCGTTTTCTTCTT
677 MAS-GG-BIK1pm-F AACAGGTCTCAGTACATTCATTTTGATTGGGATTTATCTTTTTA
678 MAS-GG-BIK1pm-R AACAGGTCTCAGTACAGACCAAAACAGTGGACTTGGG
679 MAS-GG-BPS1p-F AACAGGTCTCAACCTAAAAAGAGAGTCACTTGGGTTAAGTGATTT
680 MAS-GG-BPS1p-R AACAGGTCTCATGTTCTGATAAGTTTCAACTGAAAAAAACAAGAA
681 MAS-GG-CAD5p-F AACAGGTCTCAACCTGACTTGGGTTCAGTTAAAAATCTCA
682 MAS-GG-CAD5p-R AACAGGTCTCATGTTTTTGATGATTCTTTCTTCTTTCTTATC
683 MAS-GG-CERK1p-F AACAGGTCTCAACCTGTATGAAGAAGGGTAACAATTCAACTCTAA
684 MAS-GG-CERK1p-R AACAGGTCTCATGTTTGAAGCTTCCTTAGATTCCCCAGAGGAAGGGTGTCTGTT
685 MAS-GG-CIPP1p-F AACAGGTCTCAACCTCAAACCAGACATACTTGCAGCTTCTC
686 MAS-GG-CIPP1p-R AACAGGTCTCATGTTGAGAGTCAGATGTTCCACAAAAATCTACTC
687 MAS-GG-CIPP1pm-F AACAGGTCTCAGTTTGCAATCTGTACTAGAATAATATCGTGG
688 MAS-GG-CIPP1pm-R AACAGGTCTCAAAACGGATCTATATAACATATACGTATGCAATTAA
689 MAS-GG-CORK1p-F AACAGGTCTCAACCTGTACACTTATTAACATATATTTTTAATTTTGTG
690 MAS-GG-CORK1p-R AACAGGTCTCATGTTCGTCGACGACCAAAGATGTGAGA
691 MAS-GG-CORK1pm-F AACAGGTCTCAAGCCTGTTATTCTTAGTATTGCTTTCTATTTAAG
692 MAS-GG-CORK1pm-R AACAGGTCTCAGGCTTTAAACAATATAAAGCCCACAAG
693 MAS-GG-CPK29p-F AACAGGTCTCAACCTAATGAGGTAATGGAGGTTATCTTATCGA
694 MAS-GG-CPK29p-R AACAGGTCTCATGTTGTGAGCAAAGTAGATCGGTCTTCGA
695 MAS-GG-CPK29pm-F AACAGGTCTCAAGACACCCCCTCCAAGGGGCT
696 MAS-GG-CPK29pm-R AACAGGTCTCAGTCTCTAGGTTCTCCTATTCCTTTGCAA
697 MAS-GG-CPK5pro-F AACAGGTCTCAACCTACCATGTGACTACGACAACTACTGG
698 MAS-GG-CPK5pro-R AACAGGTCTCATGTTGAAACAATGGGAATTACCAAATCC
699 MAS-GG-CSLD2p-F AACAGGTCTCAACCTGACGACCAAGACTAGAGTTTTGGTTCG
700 MAS-GG-CSLD2p-R AACAGGTCTCATGTTAGTTAGGATCTAACTTGGCAGATCCCT
701 MAS-GG-DORN1p-F AACAGGTCTCAACCTGATGTAAAATTTGAAGCTTGAAGATGAAC
702 MAS-GG-DORN1p-R AACAGGTCTCATGTTGCAGATGATGAATCAGAGAGTCTGG
703 MAS-GG-EDS16p-F AACAGGTCTCAACCTGACTGCAGAGATCAATTTTCTTTTATTTTAT
704 MAS-GG-EDS16p-R AACAGGTCTCATGTTGCAGAAATTCGTAAAGTGTTTCTTGA
705 MAS-GG-EDS16pm1-F AACAGGTCTCACACCGCGTCCAACATTTTAAAACA
706 MAS-GG-EDS16pm1-R AACAGGTCTCAGGTGTCAGACTCTCAGCTGAACATAATT
707 MAS-GG-EDS16pm2-F AACAGGTCTCATCTGAAAGAGCCTAAGTGGGTTTCC
708 MAS-GG-EDS16pm2-R AACAGGTCTCACAGACCAGTTTTTATCATTTAAAAAATATTGTTA

bioRxiv preprint doi: https://doi.org/10.1101/2022.12.20.521163; this version posted April 18, 2023. The copyright holder for this preprint (which was not certified by peer review) is the author/funder, who has granted bioRxiv a license to display the preprint in perpetuity. It is made available under aCC-BY 4.0 International license.

709 MAS-GG-EDS1p-F AACAGGTCTCAACCTGTTTATCAGATTCCACGTACGATATGTTCTT
710 MAS-GG-EDS1p-R AACAGGTCTCATGTTGATCTATATCTATTCTCTTTTCTTTAGTGGACTTTC
711 MAS-GG-EDS1pm1-F AACAGGTCTCACGTGACCAAATCTGAAAACCCAAGT
712 MAS-GG-EDS1pm1-R AACAGGTCTCACACGTATAGAAGAAATCTACTACTTTAACTCTGTT
713 MAS-GG-EDS1pm2-F AACAGGTCTCACTCTCATGATGGGGTATTTTGGGTAAC
714 MAS-GG-EDS1pm2-R AACAGGTCTCAAGAGCATTTCAATGCAAAAATGGGT
715 MAS-GG-EFRp-F AACAGGTCTCAACCTATCTAGACGATTAAGTAATTGAGCATGTAAAAG
716 MAS-GG-EFRp-R AACAGGTCTCATGTTGTCGATTATAAAAAGATAAAAGAAAGGTTCTTCT
717 MAS-GG-ELI3p-F AACAGGTCTCAACCTTAAAGTCGATGTTCTATATGTATTCAAAATAAT
718 MAS-GG-ELI3p-R AACAGGTCTCATGTTATGGATAAATAATAAGCGAATGGGA
719 MAS-GG-ERF1p-F AACAGGTCTCAACCTCTCTCCCAATTGATATTTTTGTTATTTCT
720 MAS-GG-ERF1p-R AACAGGTCTCATGTTGTAGAAAAAATACTCTGTTTCTTGACTACTCTGT
721 MAS-GG-EX1p-F AACAGGTCTCAACCTCCGCCGTCTTAAGTGGAATTTGG
722 MAS-GG-EX1p-R AACAGGTCTCATGTTCGCCGGAGAGATGTGAGAGCG
723 MAS-GG-FERp-F AACAGGTCTCAACCTAGAAAAGTTAAGAGTGGGAACTGGGA
724 MAS-GG-FERp-R AACAGGTCTCATGTTCGATCAAGAGCACTTCTCCGG
725 MAS-GG-FH16p-F AACAGGTCTCAACCTCTGACCATAGTGTGGTAACTCAGATATTTT
726 MAS-GG-FH16p-R AACAGGTCTCATGTTGGATCAGGAACCAAACAGATGATT
727 MAS-GG-FLS2p-F AACAGGTCTCAACCTTTTTTGTTAGAGAGATTTTTGTTGTTTTTGTT
728 MAS-GG-FLS2p-R AACAGGTCTCATGTTGGTTTAGACTTTAGAAGAGTTGAAATTGTGG
729 MAS-GG-FMO1p-F AACAGGTCTCAACCTCGGAAAAATCCTTCGTCAATGTGTG
730 MAS-GG-FMO1p-R AACAGGTCTCATGTTCTGAGAGAGGTTATGCTAGAGAGAAGAGAG
731 MAS-GG-FRK1p-F AACAGGTCTCAACCTAAATTAAACGCCTTTTTATCAACAAC
732 MAS-GG-FRK1p-R AACAGGTCTCATGTTACTTAATTGAGCTGCTTTCTCTGG
733 MAS-GG-FRK1pm-F AACAGGTCTCACGTCTCTTTACATTTGTGATGTGGT
734 MAS-GG-FRK1pm-R AACAGGTCTCAGACGAACACTGATATAAAAAATCTCACA
735 MAS-GG-GLR25p-F AACAGGTCTCAACCTGATAAGAAGTGATTCAGCTGGGGTTT
736 MAS-GG-GLR25p-R AACAGGTCTCATGTTATTGATAGCTCGCAAGCTCAAATCTG
737 MAS-GG-GLR25pm-F AACAGGTCTCAACCTCTCTCACCCTGGTCGCAAA
738 MAS-GG-GLR25pm-R AACAGGTCTCAAGGTTTTCTCTTTTCAACGTACAATATTTACATGA
739 MAS-GG-GLR27p-F AACAGGTCTCAACCTCACACACTGGTCACTTAATGGTTTATTTGA
740 MAS-GG-GLR27p-R AACAGGTCTCATGTTCCAGATTGAGGAACTTTATGTCATTCTTTAAC
741 MAS-GG-GLR27pm-F AACAGGTCTCAACTCAAAATGATGCGTATCATTAATTCTATAGTTT
742 MAS-GG-GLR27pm-R AACAGGTCTCAGAGTTTGAAATTTTTAACAAAAGTCTTAAGTTATATCAG
743 MAS-GG-GPAT5p-F AACAGGTCTCAACCTAAAAAGCGTTTTAATTAGAGAGATTTTTGC
744 MAS-GG-GPAT5p-R AACAGGTCTCATGTTCTTTGTTTTTGCTCGAATATTATTTT
745 MAS-GG-HPCA1p-F AACAGGTCTCAACCTAAACATAAGAGAAAACGCAAGTTGATGA
746 MAS-GG-HPCA1p-R AACAGGTCTCATGTTCTTCAAACCCAAAAAGAACCTCTTATCA
747 MAS-GG-HRMp-F AACAGGTCTCAACCTCTGAATATCTTCTTTTGGTTGCTCTGA
748 MAS-GG-HRMp-R AACAGGTCTCATGTTCGTAATATCTCTCTGTTTTTGCTCTGTTTT
749 MAS-GG-LECRKVI2p-F AACAGGTCTCAACCTACAAAGTCAATTACTTCGAGTTTTTTTCTG
750 MAS-GG-LECRKVI2p-R AACAGGTCTCATGTTGGGTGAGCGAAGTAAAGAAGGAGATA
751 MAS-GG-LYK5p-F AACAGGTCTCAACCTATTTTCTGTTAAGTTTGAACATTTGGTTGTAA
752 MAS-GG-LYK5p-R AACAGGTCTCATGTTTTGTGGTGTTCTGATCTGAAGAGG
753 MAS-GG-LYK5pm-F AACAGGTCTCACAACAGACCAAGACCATCTTTATGTCC
754 MAS-GG-LYK5pm-R AACAGGTCTCAGTTGGATCTCATGTGAAAGAGACACATT
755 MAS-GG-LYM1p-F AACAGGTCTCAACCTATATCATCGGTAAGTCACTAGACTATTGAACG
756 MAS-GG-LYM1p-R AACAGGTCTCATGTTTTGTGTTTAGGGTTTTACGAAATTCAA
757 MAS-GG-MIK2p-F AACAGGTCTCAACCTGTAAATAACGTTGAACTCGCGG
758 MAS-GG-MIK2p-R AACAGGTCTCATGTTACAGTTGCAGATTATCTCTCTACGGTC
759 MAS-GG-MLO6p-F AACAGGTCTCAACCTAAATATACATTTGGTTGACATGTTTCTCATT
760 MAS-GG-MLO6p-R AACAGGTCTCATGTTAGAACTCACAGAACAGTTCCAAGCAAA
761 MAS-GG-MPK3p-F AACAGGTCTCAACCTAAAAAAATTCTGATCGAAAATAGCTTAC
762 MAS-GG-MPK3p-R AACAGGTCTCATGTTCTCTCTCAATTGATCAAAGTCGA
763 MAS-GG-MPK4p-F AACAGGTCTCAACCTGACTTGTTTGTGAATATAGAGGAAACATGTAATTAT
764 MAS-GG-MPK4p-R AACAGGTCTCATGTTCGGAGCAAAATTCCTCACAACAACG

bioRxiv preprint doi: https://doi.org/10.1101/2022.12.20.521163; this version posted April 18, 2023. The copyright holder for this preprint (which was not certified by peer review) is the author/funder, who has granted bioRxiv a license to display the preprint in perpetuity. It is made available under aCC-BY 4.0 International license.

765 MAS-GG-MPK6p-F AACAGGTCTCAACCTAACACAAGAGAAGAGATTTATTGCTTC
766 MAS-GG-MPK6p-R AACAGGTCTCATGTTGACCGGTAAAGATGAAAGCTTTT
767 MAS-GG-MYB15p-F AACAGGTCTCAACCTGATGAATTTGAATAAACTAAACAAAATT
768 MAS-GG-MYB15p-R AACAGGTCTCATGTTCTCTTTGATTTGTGATTGCTGATAAA
769 MAS-MYB15m-F AGAGGACCATGGACACCTGAAGAAGATCAAATCTTT
770 MAS-GG-MYB72p-F AACAGGTCTCAACCTACACGATCTCTTTTGAGATTTAAGAAG
771 MAS-GG-MYB72p-R AACAGGTCTCATGTTCTTATTACACTACTTTCTTCTCTATAGCTACC
772 MAS-GG-MYB72pm1-F AACAGGTCTCACGTTTTAAAACTTTACCTTATGTCCAATCTCT
773 MAS-GG-MYB72pm1-R AACAGGTCTCAAACGTGACGTAGCATGTGTGGGTC
774 MAS-GG-MYB72pm2-F AACAGGTCTCAGCTCTCTCTCTACGAGTGAAGTGCCT
775 MAS-GG-MYB72pm2-R AACAGGTCTCAGAGCCAAAAGCATGGAACGTACG
776 MAS-GG-NET4Ap-F AACAGGTCTCAACCTTTAATCCTCTTCTCGTACATCACAT
777 MAS-GG-NET4Ap-R AACAGGTCTCATGTTGGCTGCAAAAATCAATGGACC
778 MAS-GG-PAD4p-F AACAGGTCTCAACCTAATTAGGGTTTTATCAGATTAAAGAGATTTACTGATT
779 MAS-GG-PAD4p-R AACAGGTCTCATGTTGATTGGATATCGAGTAGAGAGTTGCAGA
780 MAS-GG-PDF12p-F AACAGGTCTCAACCTTCTACCAAAAATCTTTGGTGCTTGATC
781 MAS-GG-PDF12p-R AACAGGTCTCATGTTGATGATTATTACTATTTTGTTTTCAATGTATAGA
782 MAS-GG-PEP1p-F AACAGGTCTCAACCTGAAGTCAAAAATTGAGTCGAAAAATC
783 MAS-GG-PEP1p-R AACAGGTCTCATGTTGAGATCTGATAAGACAGAGGAAAACTT
784 MAS-GG-PEP2p-F AACAGGTCTCAACCTTGAAGCTCTTGTGAATAGAGAAGAGA
785 MAS-GG-PEP2p-R AACAGGTCTCATGTTGAAATCCAATAGTTTGGTGAGTTATC
786 MAS-GG-PEP3p-F AACAGGTCTCAACCTGCACTTTAAGTTACATTGTTTAGTCTAATTATT
787 MAS-GG-PEP3p-R AACAGGTCTCATGTTCGTTGACTTCTTAATCTTTTTTTGGGAA
788 MAS-GG-PEPR1p-F AACAGGTCTCAACCTAGAGAAGGAAAACAACCATGTATTCCAG
789 MAS-GG-PEPR1p-R AACAGGTCTCATGTTCTGAGTTTAAAGATCGAGAAACATGCAG
790 MAS-GG-PEPR1pm-F AACAGGTCTCAGAAACCAAACATCTCGTCATAAAAAAC
791 MAS-GG-PEPR1pm-R AACAGGTCTCATTTCTCTGTATACCAACGATTGTGAGA
792 MAS-GG-PEPR2p-F AACAGGTCTCAACCTAGTTTGAGATGGAGTTGCATTGTG
793 MAS-GG-PEPR2p-R AACAGGTCTCATGTTGAGATTAGAGCTCAAGAGACTGAAATAT
794 MAS-GG-PER5p-F AACAGGTCTCAACCTCAGTGCGTAGTAGTGAGTTTTCTTCA
795 MAS-GG-PER5p-R AACAGGTCTCATGTTATTTGTAGATCTCACTTGGTATATATTTCGTAC
796 MAS-GG-PER5pm-F AACAGGTCTCAGACGAATATATATAATTAGCTACTAAATTAAATT
797 MAS-GG-PER5pm-R AACAGGTCTCACGTCTCAGAACGAGTGAATGATTC
798 MAS-GG-PLP1p-F AACAGGTCTCAACCTCTGATCATCTAGCCTCTTCCC
799 MAS-GG-PLP1p-R AACAGGTCTCATGTTAATAGTTGATCGATCTTCTTTTGAGTTAA
800 MAS-GG-PMR4p-F AACAGGTCTCAACCTGCTCGATGTCGATTTGAGACGTAGT
801 MAS-GG-PMR4p-R AACAGGTCTCATGTTAGTAGCATGTGGTAGATCTTAGAAATTTCTCG
802 MAS-GG-PR1pm-F AACAGGTCTCACTCCCTCCATATAAAAAAGTTTGATTTTATAG
803 MAS-GG-PR1pm-R AACAGGTCTCAGGAGAATCATTTTATAAGTTAAAACAAGCTTG
804 MAS-GG-PR1pro-F AACAGGTCTCAACCTATATATAACGATCATTGATTAGTATATATACATATTG
805 MAS-GG-PR1pro-R AACAGGTCTCATGTTTTCTAAGTTGATAATGGTTATTGTTGT
806 MAS-GG-RALF23p-F AACAGGTCTCAACCTGGTGATTCCGGTTTCCGACG
807 MAS-GG-RALF23p-R AACAGGTCTCATGTTTCTTCTGTACACTGTAGCTTTAGCTCTCTC
808 MAS-GG-RALF23pm-F AACAGGTCTCAGAGCACTCATAATTGTACAAAATAAAAGTAAATG
809 MAS-GG-RALF23pm-R AACAGGTCTCAGCTCTCCTTCCATGATTTGAGACTATTTC
810 MAS-GG-RBOHDp-F AACAGGTCTCAACCTGACTTGTTAAATTGCTCTCTTAGTCTTA
811 MAS-GG-RBOHDp-R AACAGGTCTCATGTTCGAATTCGAGAAACCAAAAAGATC
812 MAS-GG-RBHOFp-F AACAGGTCTCAACCTACCGGTTGAAAATAAGAGTGGTGGA
813 MAS-GG-RBOHFp-R AACAGGTCTCATGTTAGATCCAAAGTCGGAATTCAAAGAGTT
814 MAS-GG-RBOHFpm-F AACAGGTCTCATGCAGAAGATAGTGAAGATAGTTGCAGAA
815 MAS-GG-RBOHFpm-R AACAGGTCTCATGCAACTTTTATAGTTTTCGAACGAAAGTA
816 MAS-GG-RCD1p-F AACAGGTCTCAACCTGGAGGAGCAGATTGGACACCGT
817 MAS-GG-RCD1p-R AACAGGTCTCATGTTCTATATATTAACAATACTAAACCTATAACCTTGATAG
818 MAS-GG-RCD1pm-F AACAGGTCTCAATACGTCTCATATAGTTATGCTGATTCTTTCTTG
819 MAS-GG-RCD1pm-R AACAGGTCTCAGTATGATCCTGTAATATCATTCCTTCACAAAA
820 MAS-GG-RFO1p-F AACAGGTCTCAACCTATATTAACCATGCATGCAAACAAA

bioRxiv preprint doi: https://doi.org/10.1101/2022.12.20.521163; this version posted April 18, 2023. The copyright holder for this preprint (which was not certified by peer review) is the author/funder, who has granted bioRxiv a license to display the preprint in perpetuity. It is made available under aCC-BY 4.0 International license.

821 MAS-GG-RFO1p-R AACAGGTCTCATGTTTTTTTTTCTCTAATGACTTTTATGTATG
822 MAS-GG-RLP26p-F AACAGGTCTCAACCTGATTAAAGGATTGATCGGTAAACAAC
823 MAS-GG-RLP26p-R AACAGGTCTCATGTTGGTGTTTGTGATTGAACCAACAAGT
824 MAS-GG-RLP29p-F AACAGGTCTCAACCTCCAGCAAAAAGCTTCTTCTACTCAA
825 MAS-GG-RLP29p-R AACAGGTCTCATGTTAGGTTTTGGTGTAAGAGAGAGGAAAGA
826 MAS-GG-RPS4p-F AACAGGTCTCAACCTCGAGAACCTTGGCGAACTTGTCA
827 MAS-GG-RPS4p-R AACAGGTCTCATGTTGGCCCAAAAGCTTTTTCCCGGT
828 MAS-GG-SCOOP12p-F AACAGGTCTCAACCTAATAGGTTTCGAGTACTGTATTGATGTTTAACTG
829 MAS-GG-SCOOP12p-R AACAGGTCTCATGTTCTCGATCTTTATTTTTTTCTCGAGTTTAGA
830 MAS-GG-SOBIR1p-F AACAGGTCTCAACCTTTTCGATTTTTCTAATCTCACAGCTGTTC
831 MAS-GG-SOBIR1p-R AACAGGTCTCATGTTTAATTAGAGAAAGTTTCTTCTTGTGGATGTT
832 MAS-GG-SULTR41p-F AACAGGTCTCAACCTATGATCCATCACACGCCTGCCT
833 MAS-GG-SULTR41p-R AACAGGTCTCATGTTGATGGCTCTTGCGCACGCTTGG
834 MAS-GG-SULTR42p-F AACAGGTCTCAACCTGTAGCTTCCACGCCCTTGCCTAA
835 MAS-GG-SULTR42p-R AACAGGTCTCATGTTCGGAATTGGTGGGATAGAGAAGAAT
836 MAS-GG-TET8p-F AACAGGTCTCAACCTCGGATGTATCAAAGGTAAAAATATC
837 MAS-GG-TET8p-R AACAGGTCTCATGTTGGTTTAGATTCAGAGAGAAAGATTG
838 MAS-GG-TUB6p-F AACAGGTCTCAACCTATTTAGAGGGTGTTATTGGTTTGTG
839 MAS-GG-TUB6p-R AACAGGTCTCATGTTCTTCTATTTTATCTGAAATCAACATTACA
840 MAS-GG-TUB6pm1-F AACAGGTCTCATAACAAAAAGTTATGAATATTCACAGACATA
841 MAS-GG-TUB6pm1-R AACAGGTCTCAGTTATGGTTAACCGAGGATGAGC
842 MAS-GG-TUB6pm2-F AACAGGTCTCAGAGGCCATTTTTTTTTCCCGT
843 MAS-GG-TUB6pm2-R AACAGGTCTCACCTCATTGCGTATGACAATGCG
844 MAS-GG-VSP2p-F AACAGGTCTCAACCTTCTCTCTGGTTATATTTTGTTGCTGCTT
845 MAS-GG-VSP2p-R AACAGGTCTCATGTTGTTTTTTATGGTATGGTTTATTGTTTAGTTTGTG
846 MAS-GG-WAKL22p-F AACAGGTCTCAACCTATATTAACCATGCATGCAAACAAA
847 MAS-GG-WAKL22p-R AACAGGTCTCATGTTTTTTTTTCTCTAATGACTTTTATGTATG
848 MAS-GG-WRKY11p-F AACAGGTCTCAACCTTAGTTCCAAAACCGCATTGACAT
849 MAS-GG-WRKY11p-R AACAGGTCTCATGTTGATGATTTCTTGGTCTGAGGATTTT
850 MAS-GG-WRKY11pm-F AACAGGTCTCAGACGAAACTGTTGATTGCTTTATTCC
851 MAS-GG-WRKY11pm-R AACAGGTCTCACGTCTCCTCAAAGTTCGAGGTTACT
852 MAS-GG-WRKY17p-F AACAGGTCTCAACCTGTCTCGCAGAGGTTATTTATCTACTTGGTT
853 MAS-GG-WRKY17p-R AACAGGTCTCATGTTGATGAGAAACCAGAGGAGAAACTTGAAG
854 MAS-GG-WRKY17pm1-F AACAGGTCTCAGGTCAACGATTCCCATGTCGCTAA
855 MAS-GG-WRKY17pm1-R AACAGGTCTCAGACCTAACCGACTAATATATATGATTGTCGTG
856 MAS-GG-WRKY17pm2-F AACAGGTCTCAAAGCAGACCAAACTTTGATTACTTTATTCCATA
857 MAS-GG-WRKY17pm2-R AACAGGTCTCAGCTTGAGTTGTGAGATATGTAGGGTCTTCTT
858 MAS-GG-WRKY33p-F AACAGGTCTCAACCTCGCTGCTTTTTCGAGATAGATAG
859 MAS-GG-WRKY33p-R AACAGGTCTCATGTTACGAAAAATGGAAGTTTGTTTTATAA
860 MAS-GG-WRKY40p-F AACAGGTCTCAACCTTGTGTATAACTATTATGCAGCCTTTTTCAA
861 MAS-GG-WRKY40p-R AACAGGTCTCATGTTGTAAATATATGTAGGATGAATCTTCGATATGGGT
862 MAS-GG-WRKY40pm-F AACAGGTCTCATACAAGAATAGGTACAGTCCTGGTTTGTG
863 MAS-GG-WRKY40pm-R AACAGGTCTCATGTAATTGTGAATAATAAAATCTTAATTCAGAT
864 MAS-GG-WRKY53p-F AACAGGTCTCAACCTATCTTGTGAGCTGATTCAAAGATTTC
865 MAS-GG-WRKY53p-R AACAGGTCTCATGTTTTAGTATATGATTCCCAAAATAGATTTTTT
866 MAS-GG-WRKY70p-F AACAGGTCTCAACCTCATTGTAGATATGATATATGAAGCTTCCCC
867 MAS-GG-WRKY70p-R AACAGGTCTCATGTTGTTAGTTTTGAGGAAGTTTTTGGTGAG
868 MAS-GG-WRKY70pm-F AACAGGTCTCAGTATCTCGCATATTAACTTAGGCTAGAGAGC
869 MAS-GG-WRKY70pm-R AACAGGTCTCAATACTATGATAAACCAGTTGGTTCTGTAGCG
870 MAS-GG-XLG2p-F AACAGGTCTCAACCTGAGTGGAGGAGCATAGTGTGATTATTTAC
871 MAS-GG-XLG2p-R AACAGGTCTCATGTTCTTCTTACCCAATCAAGCACACATACAA

bioRxiv preprint doi: https://doi.org/10.1101/2022.12.20.521163; this version posted April 18, 2023. The copyright holder for this preprint (which was not certified by peer review) is the author/funder, who has granted bioRxiv a license to display the preprint in perpetuity. It is made available under aCC-BY 4.0 International license.

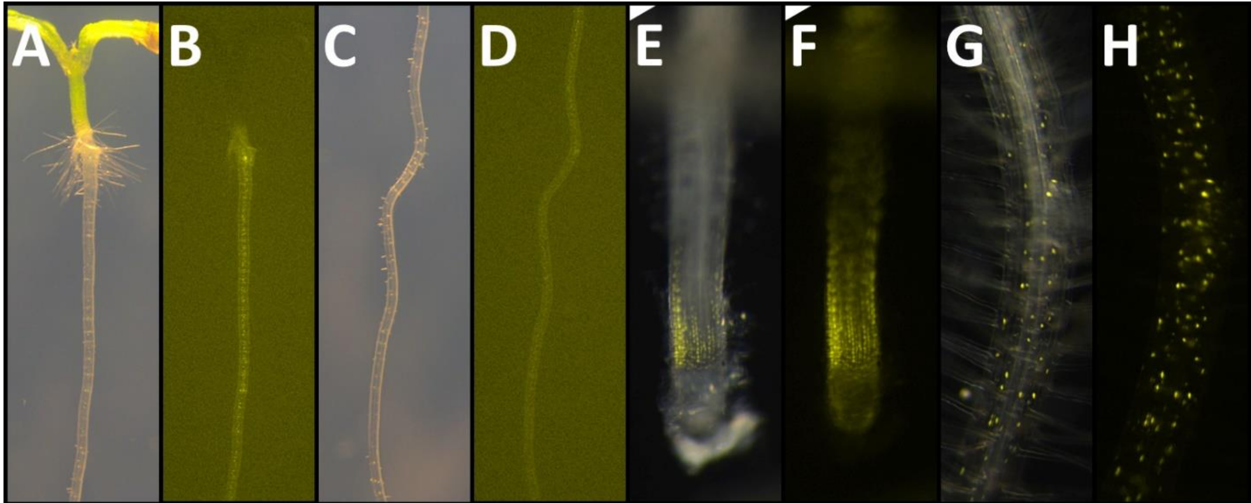

Figure S1: Expression pattern of *PEP1* and *PEP2*
A-D shows the expression of *PEP1* (yellow). Robust expression is found in the inner root tissues of the mature DZ (A, B). From the young to mature DZ, expression gradually becomes stronger (C, D). No expression in the root tip, MZ or EZ. **E-H** shows the expression of *PEP2* (yellow). Expression is found in the EZ of the tip, then disappears in the young DZ (E, F), and returns to all tissues in the mature DZ (G, H). A, C, E, G are bright field images plus fluorescence, B, D, F, H are fluorescence only.

872

bioRxiv preprint doi: https://doi.org/10.1101/2022.12.20.521163; this version posted April 18, 2023. The copyright holder for this preprint (which was not certified by peer review) is the author/funder, who has granted bioRxiv a license to display the preprint in perpetuity. It is made available under aCC-BY 4.0 International license.

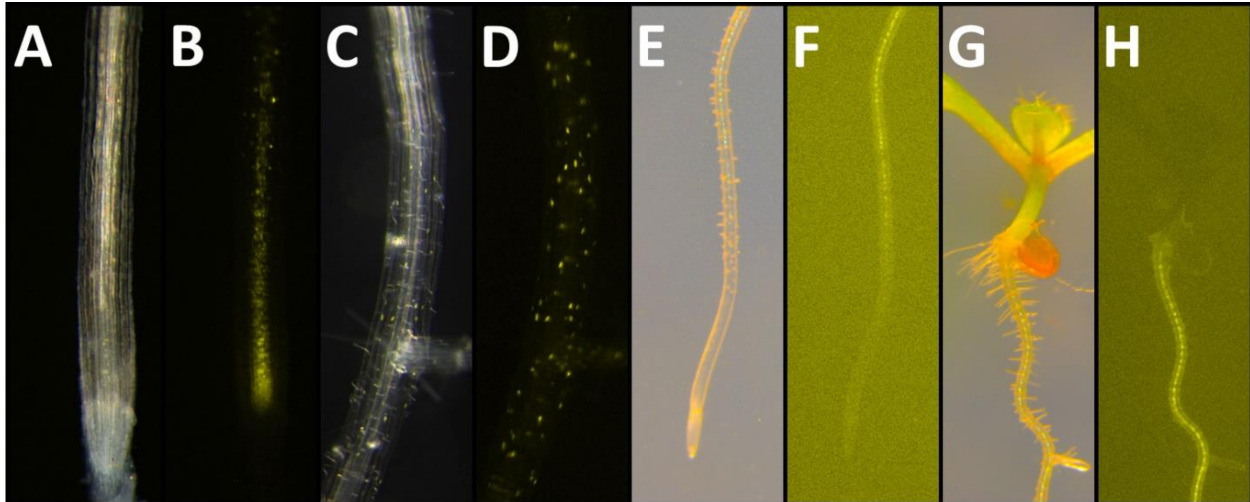

Figure S2: Expression pattern of *PEPR1* and *PEPR2*
A-D shows the expression of *PEPR1* (yellow). Weak expression is found in vasculature of the MZ, EZ and young DZ (A, B). In the mature DZ, weak expression is found in all tissues (C, D). **E-H** shows the expression of *PEPR2* (yellow). Strong expression is found in the vasculature of the DZ, starting in the root hair zone (E, F) and becoming stronger in the mature DZ (G, H). A, C, E, G are bright field plus fluorescence, B, D, F, H are fluorescence only.

873

874

bioRxiv preprint doi: https://doi.org/10.1101/2022.12.20.521163; this version posted April 18, 2023. The copyright holder for this preprint (which was not certified by peer review) is the author/funder, who has granted bioRxiv a license to display the preprint in perpetuity. It is made available under aCC-BY 4.0 International license.

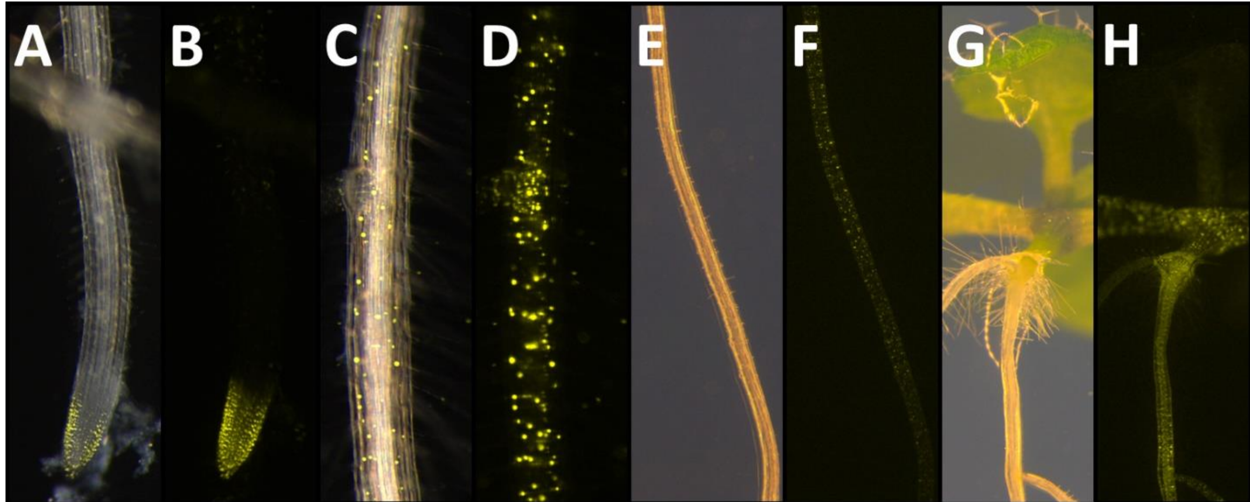

Figure S3: Expression pattern of *BIK1* and *RBOHD*
A-D shows the expression of *BIK1* (yellow). Expression is found in the root tip around the meristem, including the root cap and part of the EZ (A, B). Expression appears stronger in the outer tissues compared to the vasculature. Further up the root, expression is robust in the mature DZ, but still stronger in the outer tissues (C, D). **E-H** shows the expression of *RBOHD* (yellow). *RBOHD* is expressed in all cells and tissues from the young DZ onwards (E, F). Expression is strongest in differentiated tissue (G, H), A, C, E, G are bright field plus fluorescence, B, D, F, H are fluorescence only.

875